Master in Chemical Engineering

Hydrogen production through steam reforming of bio-oils resulting from biomass pyrolysis: Thermodynamic analysis including in situ CO_2 and/or H_2 separation

A Master's dissertation

of

Diogo Miguel Mendes Barros

Developed within the course of dissertation

held in

LEPABE - Laboratory for Process Engineering, Environment, Biotechnology and Energy

Supervisor: **Dr. Miguel Angel Soria**

Co-Supervisor: **Prof. Luís Miguel Madeira**

Departamento de Engenharia Química

July of 2017

“Time’s up, let’s do this”

-Leeroy Jenkins

Agradecimentos

Agora, na reta final da minha dissertação, resta-me agradecer a todos os que me acompanharam ao longo deste período e que fizeram com que ele se tornasse possível.

Primeiramente queria agradecer ao meu orientador, Doutor Miguel Soria, por me ajudar ao longo de toda a dissertação, por toda a ajuda e *feedback* que me deu, pelo interesse que demonstrou para com o meu o trabalho e por toda a disponibilidade que teve para comigo.

Ao meu co-orientador, Professor Luís Miguel Madeira, por ter acompanhado o desenvolvimento do trabalho e por todas as sugestões que deu para que este ficasse mais completo.

Aos meus colegas de laboratório, Cláudio e Joel, que estiveram sempre lá, ora para me tirar dúvidas, ora para tornar o ambiente de trabalho menos monótono com as suas músicas.

Aos meus amigos da FEUP que partilharam comigo estes cinco anos e fizeram com que eles valessem bem a pena; e em particular ao BDC, por serem aquela má influência que me leva a procrastinar, mas que fazem sempre uma pessoa rir-se.

Ao pessoal de Matosinhos, Catarina, Miguel e Sofia, que me conhecem desde miúdo, mas ainda assim têm sempre vontade e disponibilidade para tomar um café comigo.

E por fim à minha família, aos meus pais que me suportaram, me ensinaram muito do que sei e sempre apoiaram as minhas decisões. Aos meus tios que se importam bastante comigo e são sempre curiosos sobre o que ando a fazer na faculdade, ao meu primo Luís que daqui a pouco também será engenheiro e às minhas avós que se preocupam demasiado e para as quais só me alimento bem se estiver a comer em casa delas.

Este trabalho foi financiado por: Projeto POCI-01-0145-FEDER-006939 - Laboratório de Engenharia de Processos, Ambiente, Biotecnologia e Energia – LEPABE - financiado pelo Fundo Europeu de Desenvolvimento Regional (FEDER), através do COMPETE2020 – Programa Operacional Competitividade e Internacionalização (POCI) e por fundos nacionais através da Fundação para a Ciência e a Tecnologia I.P.

Resumo

Nesta dissertação foi feita uma análise termodinâmica baseada no método da minimização da energia livre de Gibbs de forma a estudarem-se os processos de reformação a vapor de bio-óleos (óleos provenientes da pirólise de biomassa) de diferentes origens. A dissertação tem por objetivo demonstrar a viabilidade da produção de hidrogénio com elevada pureza a partir destes bio-óleos. Os cálculos da composição de equilíbrio forma realizados recorrendo-se ao *software* Aspen Plus®. Num reator convencional, esta análise foi realizada numa gama de temperaturas de 100 a 1200 °C e para razões molares água/bio-óleo (WFR) de 1 a 15, sempre à pressão de 1 bar. Todos os bio-óleos testados mostraram um comportamento semelhante relativamente à influência da temperatura e do WFR; escolheram-se os bio-óleos capazes de produzirem o rendimento de H_2 mais elevado (trigo - 11,94 mol H_2/mol de bio-óleo) e um dos rendimentos mais baixos (abeto - 4,75 mol H_2/mol de bio-óleo) de modo a estudar o seu potencial em diferentes configurações de reator.

Posteriormente foram analisadas outras configurações de reatores com separação *in-situ* de CO_2 e H_2. A captura do CO_2 foi simulada numa gama de razão molar de adsorvente (CaO)/bio-óleo (SFR) de 0 a 6 enquanto a remoção de H_2 foi simulada com o uso de uma fração de remoção de 0 a 0,8 (valores típicos de recuperação numa membrana seletiva ao H_2). Foram também encontradas as condições em que o processo é energeticamente neutro, variando-se a quantidade de adsorvente.

As condições ótimas para a produção de hidrogénio foram obtidas no reator com remoção combinada de H_2 e CO_2 (*sorption-enhanced membrane reactor* – SEMR) no qual foi possível obter 99% do rendimento teórico máximo para o abeto e 97% do rendimento máximo para o trigo. Estas condições foram obtidas a 400 °C, $WFR = 6$, $SFR = 2$, $fH_2 = 0{,}8$ e 1 bar para o abeto e 400 °C, $WFR = 10$, $SFR = 5$, $fH_2 = 0{,}8$ e 1 bar para o trigo. Além disso, esta configuração minimiza o rendimento de CH_4, CO, CO_2 e coque. Estas condições ótimas requerem mais CaO do que é necessário para o processo ser energeticamente neutro.

Além disso, foi também simulado o efeito da pressão numa gama de 1 a 10 bar para as configurações do reator com remoção de H_2, uma vez que, em condições experimentais, quanto maior a força-motriz, maior será o H_2 permeado através da membrana (i.e., na prática, é irrealista obter frações de remoção de 80% a operar a 1 bar). Foi demonstrado que o aumento da pressão diminui o rendimento de H_2; no entanto, isto pode ser ultrapassado com o aumento de WFR.

Palavras-chave: Bio-óleo; Reformação a vapor; Hidrogénio; Reator de adsorção; Reator com membrana; Reator combinado com adsorção e membrana.

Abstract

In this dissertation, a thermodynamic analysis based on the minimization of the Gibbs free energy method was applied in order to study the steam reforming of bio-oils (oils from biomass pyrolysis) from different sources. The aim of the dissertation is to demonstrate the feasibility of producing high-purity hydrogen from these bio-oils. Calculations of the chemical equilibrium compositions were performed using Aspen Plus® software. In a conventional reactor, this analysis was carried out at for a temperature range of 100 to 1200 ºC and water to feed molar ratio (WFR) from 1 to 15, always at a pressure of 1 bar. All the bio-oils assessed showed a similar behaviour with respect to the influence of temperature and WFR; those bio-oils able to produce the highest (wheat - 11.94 H_2 mol/bio-oil mol) and one of the lowest (spruce - 4.75 H_2 mol/bio-oil mol) H_2 yields were chosen to study their potential in different reactor configurations.

Multifunctional reactors with in situ separation of CO_2 and/or H_2 were analysed. The CO_2 capture was simulated varying the sorbent (CaO) to feed molar ratio (SFR) in a range of 0 to 6 while the H_2 removal with the use of a removal fraction of 0 to 0.8 (typical recoveries for an H_2-selective membrane). The neutral energy conditions were also found, varying the adsorbent ratio.

The optimum conditions for the production of hydrogen were obtained in the reactor with combined removal of H_2 and CO_2 (sorption-enhanced membrane reactor – SEMR) in which it was possible to obtain 99% of the maximum theoretical yield for spruce bio-oil and 97% of the maximum yield for wheat bio-oil. These conditions were obtained at 400 °C, WFR = 6, SFR = 2, fH_2 = 0.8 and 1 bar for spruce and 400 °C, WFR = 10, SFR = 5, fH2 = 0.8 and 1 bar for wheat. Furthermore, this reactor configuration minimizes CH_4, H_2, CO, CO_2 and coke yield. These optimum conditions require more CaO than what is necessary for the process to be energetically neutral.

In addition, the effect of pressure in a range of 1 to 10 bar was also accessed for the reactor configurations with H_2 removal since, in experimental conditions, the higher the H_2-driving force is, the higher will be the H_2 recovered through the membrane (i.e., in practice operating at 1 bar would be unrealistic to reach recoveries as high as 80%). It was shown that the increase of pressure decreases H_2 yield; yet, this can be overcome by the increase of WFR.

Keywords: Bio-oil; Steam reforming; Hydrogen; Sorption-enhanced reactor; Membrane reactor; Sorption-enhanced membrane reactor.

Declaration

I hereby declare, on my word of honour, that this work is original and that all non-original contributions were properly referenced with source identification.

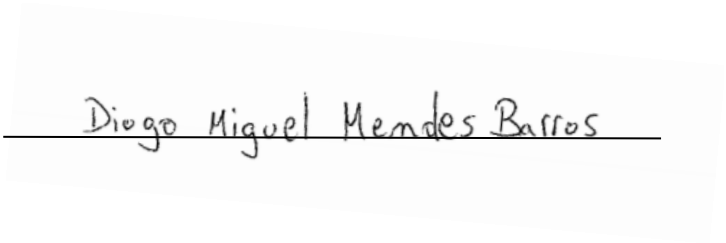

03 of July of 2017

Index

Notation and Glossary

Latin and Greek letters

Symbol	Unit	Definition
A	[-]	Number of atoms in the species
B	[-]	Number of atoms in the feed
F	[-]	Removal fraction
$\hat{f}$	[atm]	Fugacity
N	[kmol]	Number of moles
M	[kmol/h]	Molar flow rate
V	[m^3/mol]	Molar volume
Y	[-]	Mole fraction
G	[kJ/mol]	Gibbs free energy
ΔG_f	[kJ/mol]	Gibbs free energy of formation
ΔH_r^{298K}	[kJ/mol]	Standard enthalpy of reaction
P	[atm]	Pressure
R	[J/(kmol.K]	Ideal gas universal constant
S	[J/K]	Entropy
T	[K]	Temperature
V	[m^3]	Volume
λ	[-]	Lagrangian multiplier
μ	[J/mol]	Chemical potential
ϕ	[-]	Fugacity coefficient
ω	[-]	Acentric factor

Index

Index	Definition
$( )^0$	Standard Conditions
$( )_i$	Chemical species i
$( )_j$	Atom j
$( )_C$	Critical conditions
$( )_r$	Reduced
$( )_T$	Total

Acronyms

Acronyms	Definition
MR	Membrane Reactor
SER	Sorption-Enhanced Reactor
SEMR	Sorption-Enhanced Membrane Reactor
SFR	Sorbent to Feed Ratio
SR	Steam Reforming
WGS	Water-Gas Shift
WFR	Water to Feed Ratio
RWGS	Reverse Water-Gas Shift
sq	Stoichiometric

Chemical Abbreviations

Molecular formula	Name
Ag	Silver
C	Carbon
CH_4	Methane
C_2H_6	Ethane
C_4H_{10}	Butane
CH_4O	Methanol
$C_4H_{10}O$	Butanol
$C_nH_mO_k$	Oxygenated compound
$CaCO_3$	Calcium carbonate
CaO	Calcium oxide
$Ca(OH)_2$	Calcium hydroxide
H_2	Hydrogen
H_2O	Water
MgO	Magnesium oxide
NaOH	Sodium oxide
Ni	Nickel
Pd	Palladium
Pt	Platinum
Rh	Rhodium
Ru	Ruthenium

1 Introduction

1.1 Framing and presentation of the work

In present times, the non-sustainable consumption of fossil-fuels coupled with the environmental threats created by their exploitation is a growing concern for the society. This has led to an increasing demand for clean and renewable energy sources like biofuels.

Biomass is seen as an attractive primary energy source (renewable resource) if managed in a sustainable way – it can be converted in a large array of biofuels through several processes, and the combustion of these biofuels has low carbon emissions. Considering the carbon life-cycle, these fuels can be considered to have little to no CO_2 emissions as this gas was previously absorbed by the plants that originated the biomass [1].

Biomass is the name given to the biodegradable fraction of residues from agriculture, forest management and other forestry activities, as well as the biodegradable fraction from industrial or urban wastes. It can be divided in terms of its origin as natural or anthropogenic. The natural biomass comes from the forests ant their residues, the anthropogenic one comes from agricultural, municipal and industrial wastes (e.g. paper or food industry) – caused or produced by humans. It can also be divided in terms of its chemical composition into oleaginous (from sunflowers, soy, etc.), containing starch (from cereals), sugary (bagasse from sugar cane, beetroots) or lignocellulosic (containing cellulose, hemicellulose and lignin and typically comes from woods) [2].

As above stated, biomass can be turned into different kinds of fuels and this can be done through thermal, biological and mechanical processes. The different transformation routes that biomass can suffer are presented in Figure 1.1. The thermal processes are comprised by combustion, gasification, and pyrolysis. The biological processes consist of fermentation or anaerobic digestion that originate ethanol or bio-gas respectively. The mechanical processes entail the extraction of oils of seeds that can later be used in the production of bio-diesel.

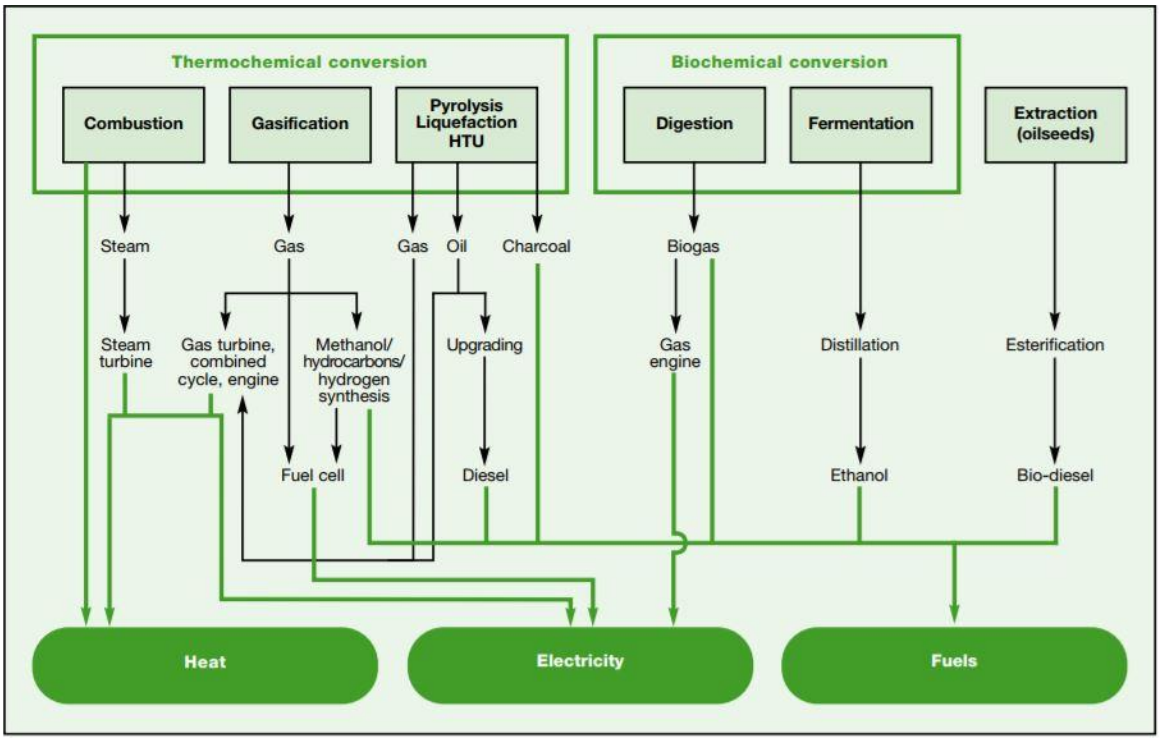

Figure 1.1 - Main Biomass energy coversion routes [3].

Focusing on the thermal processes, combustion is used in the production of heat that can be used to generate electrical energy (e.g. using a stream of steam that makes a turbine spin). Gasification is mainly used to produce syngas, which is a gas mixture of mostly H_2 and CO and some other gases as CO_2 and CH_4 that have different downstream applications [4]. Pyrolysis is the thermal decomposition of the biomass in the absence of oxygen; it creates charcoal, fuel-gas and bio-oil, also called pyrolysis oil, the quantity in which these products are formed as well as their content on oxygenated compounds depends on the retention time and temperature of the process and on the composition of the biomass source [5]. In Table 1.1 are represented the average yields of the products obtained through gasification and different varieties of pyrolysis.

The flash or fast-pyrolysis is the one which has a bigger yield in bio-oil, while the other sub-products (charcoal and fuel-gas) can be used to generate heat for the pyrolysis process itself [6]. The big advantage of producing these bio-oils is that they have a volumetric energy density up to ten times higher than that of biomass; consequently they are much more suited (more cost-efficient) for transportation [7]. These oils can be used directly as combustion fuels, but their poor volatility and high viscosity and coking result in problems for the combustion equipment. They can also be used to extract some chemicals like acetic acid or methanol, but these compounds can usually be obtained at a lower cost from other feedstocks. Finally, they can be converted to

transport fuels like bio-diesel or hydrogen; even though there are still some challenges, this is an attractive application for bio-oils [8].

Table 1.1 - Typical product yields (dry wood basis) obtained by different modes of pyrolysis of wood [6].

Mode	Conditions	Liquid (%)	Char (%)	Gas (%)
Fast	Moderate temperature, around 500 °C, short hot vapour residence time, ~1 s	75	12	13
Intermediate	Moderate temperature, around 500 °C, moderate hot vapour residence time ~10–20 s	50	20	30
Slow (carbonisation)	Low temperature, around 400 °C, very long residence time	30	35	35
Gasification	High temperature, around 800 °C, long residence times	5	10	85

Hydrogen is a great energy solution as it has a high calorific power and also acts as an excellent energy vector. Nowadays, 95% of the world's production of hydrogen uses fossil fuels as raw material [9], mainly through methane steam reforming. However, the use of this technology for the reforming of pyrolysis oils is particularly interesting because not only it is an environmentally friendly alternative, but also, it is an application that can turn a product that is otherwise viewed as waste (biomass) into a useful fuel. This is the topic that will be explored along this dissertation.

1.2 Organization of the thesis

The dissertation is organized as follows:

In Chapter 1 it is given the contextualization of the work that will be carried throughout the dissertation.

In Chapter 2 the steam reforming processes for hydrogen production, conventional and alternative reactor configurations as well as previous studies performed in steam reforming of oxygenated compound are described.

In Chapter 3, the methodology used to calculate the thermodynamic equilibrium compositions (via steam reforming of bio-oils resulting from biomass pyrolysis), and the assumptions that were made for the simulations, are stated.

In Chapter 4 the results obtained from the simulations in different reactor configurations are presented and discussed for the different parameters evaluated (temperature, water to feed ratio, pressure, sorbent to feed ratio in a sorption-enhanced reactor and hydrogen removal fraction in a membrane reactor).

In Chapter 5, the conclusions obtained from this work are presented in addition to future work that can be carried out in this subject.

2 Context and State of the art

2.1 Steam Reforming

Steam reforming (SR) is a process that can be used to obtain hydrogen, by mixing a feed of hydrocarbons or oxygenated compounds (e.g. bio-oil derived from biomass pyrolysis) with water (steam). The feed is converted into synthesis gas through the steam-reforming reaction – Eq. (2.1). These type of reactions are endothermic, which means that heat needs to be supplied for the reactions to proceed [10]. Following this step, carbon monoxide is converted to hydrogen and carbon dioxide through the water-gas shift (WGS) reaction Eq. (2.2), which is exothermic.

$$C_nH_mO_k + (n-k)H_2O \leftrightharpoons nCO + \left(n + \frac{m}{2} - k\right)H_2 \quad (2.1)$$

$$CO + H_2O \leftrightharpoons CO_2 + H_2 \quad (2.2)$$

Thus, the sum of both reaction results in the overall steam reforming equation that can be represented as follows [11]:

$$C_nH_mO_k + (2n-k)H_2O \leftrightharpoons nCO_2 + \left(2n + \frac{m}{2} - k\right)H_2 \quad (2.3)$$

As it is shown through the SR equation, the higher the number of hydrogen atoms in the oxygenated compound, the higher the hydrogen yield (defined as the molar ratio of H_2 produced per oxygenated compound in the feed) will be; so it is an advantage to work with bio-oils instead of natural gas, since they typically have much more complex compounds, which have a higher number of hydrogen atoms [12]. The possible reactions for bio-oil steam reforming are presented in table 2.1; these reactions were considered based on previous studies conducted for the steam reforming process [13-15].

Table 2.1 – Reactions considered for the reforming process simulations

Reaction	ΔH_r^{298K}(kJ mol^{-1})	No.
Steam Reforming		
$C_nH_mO_k + (n-k)H_2O \rightarrow nCO + \left(n + \frac{m}{2} - k\right)H_2$	>0	(2.1)
Water-gas shift		
$CO + H_2O \leftrightharpoons CO_2 + H_2$	-41	(2.2)

Thermal decomposition of oxygenated compounds		
$C_nH_mO_k \leftrightarrows H_2, CO,$ smaller oxygenated compounds, hydrocarbons, coke ...	>0	(2.4)
Methanation		
$CO + 3H_2 \leftrightarrows CH_4 + 2H_2O$	-206	(2.5)
Methane steam reforming		
$CH_4 + H_2O \leftrightarrows 4H_2 + CO_2$	-165	(2.6)
Methane dry reforming		
$CH_4 + CO_2 \leftrightarrows 2CO + 2H_2$	247	(2.7)
Carbon Formation		
$2CO \leftrightarrows CO_2 + C$	-172	(2.8)
$CH_4 \leftrightarrows 2H_2 + C$	75	(2.9)
$CO + H_2 \leftrightarrows H_2O + C$	-131	(2.10)
$CO_2 + 2H_2 \leftrightarrows 2H_2O + C$	-90	(2.11)

Thermodynamically, the steam reforming process is mainly affected by the temperature, the steam to carbon molar ratio and the total pressure. It is favoured by high temperatures, low pressures and an excess of steam [9, 16]. There are also concerns associated with this process that are the secondary reactions that form by-products such as CO, CO_2, CH_4 and coke. This last species is particularly critical as it can lead to the catalyst deactivation, as was observed in an experimental study of steam reforming of bio-oil aqueous fraction over Ni/La_2O_3–αAl_2O_3 catalyst [11]. The CO acts as a poison for most fuel-cells applications [13], and so its formation should be avoided for such end-use. Thermodynamic studies have been conducted for steam reforming of acetic acid (which is usually a main component in wood bio-oils [17]) and bio-oils [12, 13, 18] in a conventional reactor. It was concluded that the temperature is the most influential parameter in the product equilibrium since its increment favours the endothermic SR reaction, but will also hinder the WGS, reduce the coke formation and the methanation reaction. Steam to carbon ratio is the second most important parameter – an excess of steam can improve the H_2 yield and reduce both coke and CH_4 formation, since the presence of complex oxygenated compounds increases the probability of coke formation. Finally, high pressures lead to a decrease in the H_2 formation, which is justified according to Le Chatelier's principle. During the steam reforming process, the number of moles will vary and higher pressures will shift the thermodynamic equilibrium of the SR (eq. 2.3) and the methanation reaction (eq.2.5) towards the production of a lower number of moles,

thus inhibiting H_2 production. Because of that the use of atmospheric pressure is recommended in conventional reactors.

Furthermore, experimental studies conducted with both bio-oil and bio-oil model compounds like acetic acid, showed that catalytic bio-oil steam reforming is a viable technology [19]. Studies were carried out with acetic acid and bio-oil in order to access which catalyst would be more suitable for this reaction. It was stated that even though Rh (rhodium), Ru (ruthenium) and Pt (platinum) based catalyst are active and stable, the high price limits their industrial application. On the other hand, Ni (nickel) based catalyst also proved to be active and have low costs, yet, are susceptible to coke formation which will lead to catalyst deactivation [20, 21].

To minimize the formation of coke and CH_4 in the reaction zone and to maximize the H_2-yield, high temperatures and a high steam to feed ratio need to be used. However, these conditions can turn out to be very expensive, and so other alternatives to overcome these limitations can be explored, like using a different reactor configuration that provide the possibility of employing milder temperatures and less steam. Such reactor configurations will be presented in the sub-chapters bellow.

2.2 Sorption-enhanced Reactor

According to the Le Chatelier's principle, the removal of CO_2 (a reaction product) from the reaction zone will cause a shift of the equilibrium in the overall steam reforming reaction (Eq. 2.3) to the side of further hydrogen production; however, this will also result in a reduction of CH_4 and CO through an equilibrium shift in the secondary reactions (Eqs. 2.2, 2.6). This removal can be achieved by filling the reactor with a mixture of steam reforming catalyst and CO_2 sorbent, turning it into a sorption-enhanced reactor (SER) as shown in Figure 2.1.

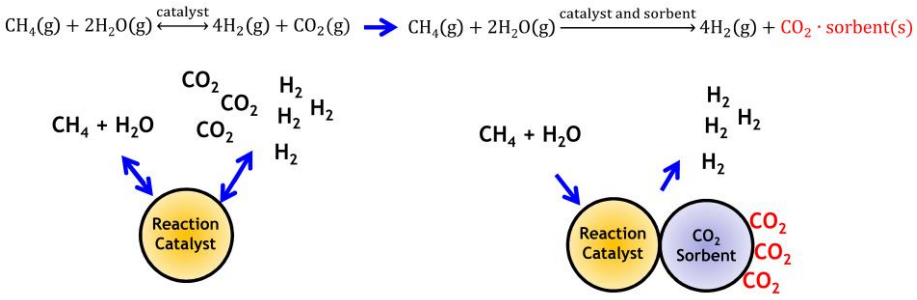

Figure 2.1 – H_2 production from conventional methane steam reforming vs sorption-enhanced methane reforming. Copyright 2017, World Scientific Publishing [22].

The most common adsorbent used for CO_2 capture in a SER is calcium oxide (CaO), which has previously been used in theoretical glycerol reforming studies and in experimental acetic acid reforming, employed as a bio-oil model compound [23], [24]. Alternatives to this sorbent are sodium hydroxide (NaOH) [23], magnesium oxide (MgO) [25] and hydrocalcite [26]. The reactions that describe the carbon dioxide sorption are represented in Table 2.2 for the CaO case.

Table 2.2 - Carbon dioxide sorption reactions involved in its capture with calcium oxide.

Reaction	ΔH_r^{298K}(kJ mol^{-1})	No.
$CaO + H_2O \leftrightharpoons Ca(OH)_2$	-65	(2.12)
$Ca(OH)_2 + CO_2 \leftrightharpoons CaCO_3 + H_2O$	-113	(2.13)

The use of a SER with CaO as sorbent demonstrated the increase of H_2 yield when compared to a normal SR reactor in the thermodynamic studies for both glycerol steam reforming and glycerol autothermal reforming by Silva et al. [27] and Leal et al. [14], respectively. Moreover, the CO_2 sorption may also suppress the formation of coke; this is quite important aspect for bio-oil reforming as the chemical oxygenated species are more complex, which can give rise to a higher coke formation [28].

2.3 Membrane Reactor

Another option to promote a shift in the steam reforming reaction to the side of the reaction products is through the in-situ separation of hydrogen. For this a selective membrane might be employed, as illustrated in Figure 2.2.

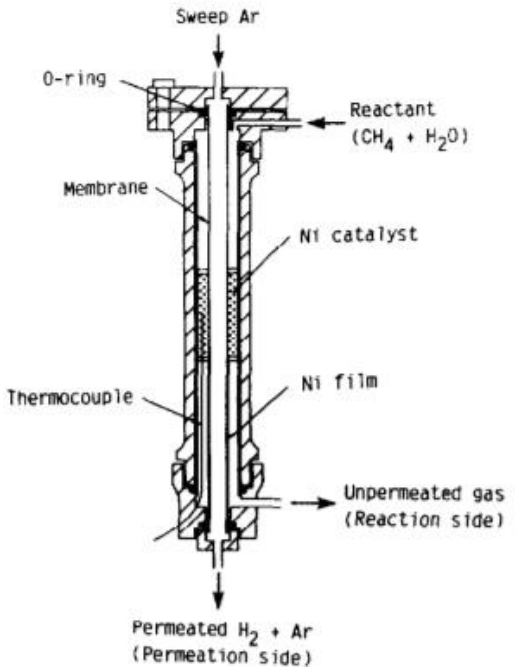

Figure 2.2 - Structure of hydrogen-permeable membrane reactor [29].

Palladium-based membranes have been largely studied and applied in hydrogen separation/production processes, since they are very selective towards H_2 [30]. Even though pure palladium membranes have a high selectivity, their commercialization is limited due to their elevated costs and the embrittlement phenomenon. Because of this, palladium alloys comprising another metal, for instance, silver, are used; these alloys improve the chemical resistance of the membrane and also its hydrogen permeability [31]. Besides chemical resistance and cost, temperature of operation should also be considered for the industrial application of these membranes. An increase of temperature will lead to an increase in the membrane permeability but only until a certain point; above that permeability decreases irreversibly due to the formation of inter-metallic compounds or membrane damage, and for this reason the palladium-based membrane reactor (MR) should not operate in a temperature superior to values around 550 °C [32].

There are thermodynamic studies available in the literature regarding hydrogen removal in glycerol steam reforming processes [14, 27, 33]. These studies showed that with hydrogen removal the H_2 yield increased, even allowing to achieve the maximum possible theoretical conversion (7 moles of H_2 per mole of glycerol fed) for hydrogen removal fractions above 0.99, while also inhibiting the methanation reaction. However, this value of hydrogen removal/recover might not be experimentally feasible. Furthermore, in the MR, higher hydrogen removal fractions lead to a decrease in the temperature for which the maximum yield is obtained, thus providing an opportunity to operate under milder reaction conditions. An experimental study carried out for acetic acid that aimed to evaluate the hydrogen selectivity and yield with a Pd-Ag membrane,

showed that the MR provided better results than the traditional steam reforming reactor (increasing from a yield of 34.2% to 43.4% at 1.5 bar) [34].

2.4 Sorption-enhanced membrane reactor

The simultaneous removal of CO_2 and H_2 from the reaction zone provides a hybrid new reactor concept that originates a substantial improvement in the hydrogen yield. Silva et al. [27], working with glycerol, showed through thermodynamic studies that for the sorption-enhanced membrane reactor (SEMR), the maximum theoretical conversion can be obtained even without the need of operating with a hydrogen removal fraction of 0.99, but instead using a more realistic recovery fraction of 0.8. It was also demonstrated an improvement of 47% and 22% when compared to the SER and the MR, respectively.

Experimentally, the SEMR has been tested for the WGS reaction using hydrocalcite as CO_2 sorbent [26]. It was demonstrated that the use of this reactor configuration increased the conversion of CO, when compared with the traditional reactor and the SER, leading to the production of a H_2 stream with high purity.

For a hypothetical industrial application of the SER and SEMR, some issues should be taken into account, mainly concerning the regeneration of the sorbent and its operation time. For an effective use of the these reactor configurations, at least two parallel reactors should be needed, working in a cyclic manner: while one will be producing H_2 through the SR reaction the other will be regenerating the sorbent [27]. Once the first one is saturated, they will switch the roles. This is illustrated in Figure 2.3.

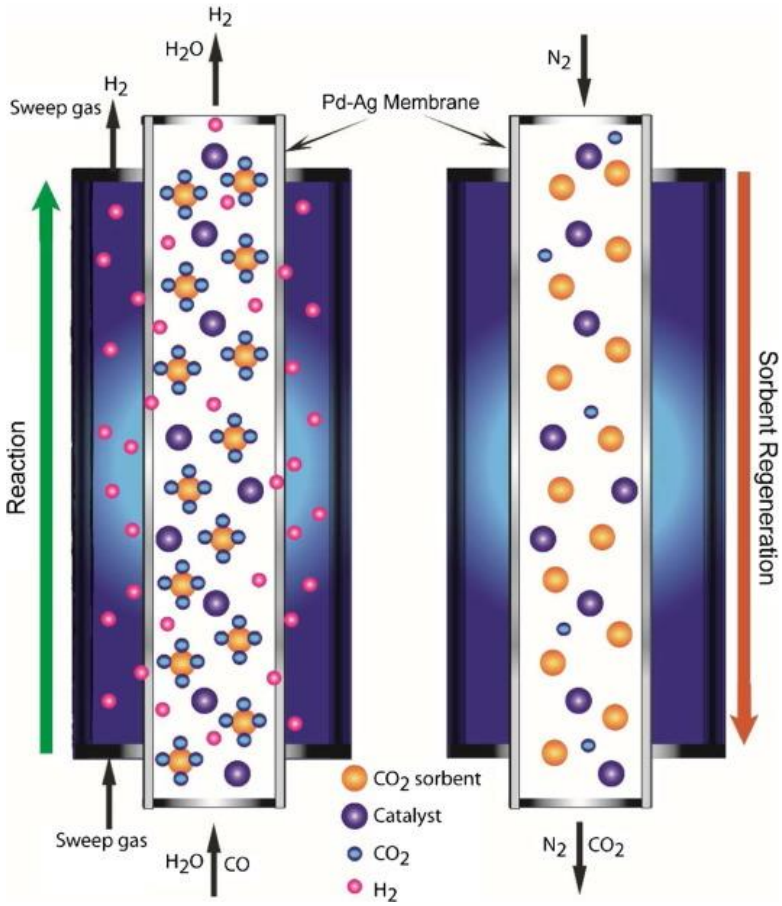

Figure 2.3 – Schematic view of the SEMR based on 2 parallel reactors configuration for continuous operation.

2.5 Work's purpose

The purpose of this thesis is to further explore biomass valorisation, namely through the steam reforming of pyrolysis oils. For comparison reasons, several fractions of bio-oil derived from biomass pyrolysis whose composition depends on the sources (e.g. wood, sugar, palm oil, etc.) are used. This work focuses on the thermodynamic equilibrium analysis of the steam reforming process as well as on the effect of important operating parameters such as temperature, pressure, feed composition and steam to feed molar ratio on the hydrogen yield as well as on the yield of undesired sub-products (e.g. CO, CH_4 and coke).

Moreover, different reactor configurations, with in-situ carbon dioxide or hydrogen removal are addressed, as these configurations may improve the hydrogen yield without the need of employing high temperatures or steam to feed molar ratios. This will also create the necessity of evaluating the effect of additional parameters, which are the sorbent to feed ratio (for the CO_2 removal) and the hydrogen removal fraction (for the H_2 removal through the membrane). The

different reactor configurations such as traditional reactor, membrane reactor, sorption-enhanced reactor and sorption-enhanced membrane reactor will be compared with the aim of identifying the optimal operating conditions for high-purity hydrogen production. Although these conditions correspond to the equilibrium, they provide valuable information for operation under real conditions since they indicate the limits that can be reached and the variables that can be modified in order to optimize the hydrogen yield and avoid (or minimize) the coke formation, which is responsible for catalyst deactivation.

3 Methodology

To determine the equilibrium composition of the chemical species in the system, a non-stoichiometric approach was employed. This approach involves the minimization of the Gibbs free energy and allows for an easy achievement of convergence in computation without the need to select the chemical reaction(s) occurring and an accurate estimation of the initial equilibrium composition, only needing to define the chemical species involved according to the possible reaction(s) [35].

The Gibbs free energy (*G*) depends on the temperature (*T*), pressure (*P*) and molar quantities of the *N* components in the system. Its differential form can be written as follows:

$$dG = -SdT + VdP + \sum_{i=i}^{N} \mu_i dn_i \tag{3.1}$$

where *S* is the entropy, *V* the volume, n_i the number of moles of each component in the system and μ_i is the respective chemical potential. When the system operates in isothermal and isobaric conditions, the differential equation becomes:

$$dG = \sum_{i=i}^{N} \mu_i dn_i \tag{3.2}$$

Since the minimization of the Gibbs free energy is being used and this minimum is reached at equilibrium, the used approach implies that equation (3.2) equals zero. From that, the total Gibbs free energy can be written as:

$$G = \sum_{i=i}^{N} \mu_i n_i = \sum_{i=i}^{N} n_i G_i^0 + RT \sum_{i=i}^{N} n_i ln\left(\frac{\hat{f}_i}{f_i^0}\right) \tag{3.3}$$

where G_i^0 is the standard Gibbs free energy for each species and $\hat{f}_i$ and f_i^0 are the fugacity and standard-state fugacity of each species in the system respectively. G_i^0 is assumed to be zero for every component in its standard state. In addition, for equilibrium state in gas phase, $\hat{f}_i$ can be given by equation (3.4), while $f_i^0 = P^0$.

$$\hat{f}_i = \hat{\phi}_i y_i P \tag{3.4}$$

In these equations, y_i stands for the molar fraction of component *i*, while *P* and P^0 are the pressure of the system and the standard-state pressure of 1 atm, respectively. $\hat{\phi}_i$ represents the fugacity coefficient of the gas mixture, which can be calculated resorting to the Soave-Redlich-Kwong

equation of state (Appendix A) [36]. This method is appropriate for nonpolar or moderately polar mixtures (e.g. methane, hydrogen and carbon dioxide) and for processes operating with high temperatures [27].

Introducing elemental balances constraints and Lagrangian multipliers, λ_i, the function *G* can be rewritten as G' (3.6)

$$\sum_{i=1}^{N} a_{ji} n_i = b_j\,, \qquad j = 1, \dots, M \tag{3.5}$$

$$G' = \sum_{i=1}^{N} n_i G_i^0 + RT \sum_{i=1}^{N} n_i \ln\left(\frac{\hat{\phi}_i y_i P}{P^0}\right) + \sum_{j=1}^{M} \lambda_i \left(\sum_{i=1}^{N} a_{ji} n_i - b_j\right) \tag{3.6}$$

where a_{ji} represents the number of atoms *j* in the species *i* and b_j is the total number of atoms *j* in the feed. In order to find the equilibrium composition at its minimum energy value, the derivative of G' with respect do n_i must be zero, which leads to the equation bellow:

$$\left(\frac{\delta G'}{\delta n_i}\right)_{T,P,n_j \neq i} = \Delta G_{fi}^0 + RTln\left(\frac{\hat{\phi}_i y_i P}{P^0}\right) + \sum_{j=1}^{M} \lambda_i a_{ji} = 0\,, \qquad i = 1, \dots, N \tag{3.7}$$

or

$$\frac{\Delta G_{fi}^0}{RT} + \ln\left(\frac{P}{P^0}\right) + \ln\left(\hat{\phi}_i\right) + \ln\left(\frac{n_i}{n_T}\right) + \sum_{j=1}^{M} \frac{\lambda_i a_{ji}}{RT} = 0\,, \qquad i = 1, \dots, N \tag{3.8}$$

n_T representing the total number of moles of all species and is defined by:

$$n_T = \sum_{i=1}^{N} n_i \tag{3.9}$$

Equations (3.7), (3.8) and (3.9) represent a non-linear system with $M + N + 1$ equations which can be solved to find the unknown variables n_i, λ_i and y_i at equilibrium.

When the presence of solid-phase carbon (graphite) is considered, its standard Gibbs energy, $G_{C(s)}^0$, is considered to be zero [36]. Though, for an isothermal process:

$$dG_{C(s)}(T, P) = V_C dP \tag{3.10}$$

V_C being the mole volume of solid-phase carbon, which can be considered a constant since it is less affected by temperature and pressure. The step integration of Eq. (3.10) can be seen in Eqs. (3.10) and (3.11):

$$G_{C(s)}(T,P) - G_{C(s)}(T,P^0) = V_C(P - P^0) \tag{3.11}$$

$$G_{C(s)}(T,P) = V_C(P - P^0) \tag{3.12}$$

Thus, considering the presence of solid-phase carbon in the system, equation (3.8) becomes

$$\frac{\Delta G_{fi}^0}{RT} + \ln\left(\frac{P}{P^0}\right) + \ln(\hat{\phi}_i) + \ln\left(\frac{n_i}{n_T}\right) + \sum_{j=1}^{M} \frac{\lambda_i a_{ji}}{RT} + \frac{n_C G_{C(s)}}{RT} = 0\,, \qquad i = 1, \dots, N-1 \tag{3.13}$$

The thermodynamic analysis of the different bio-oils in the steam reforming process was performed using Aspen Plus® V8.8 software, with the objective of studying the influence of T, P and feed composition on the hydrogen yield. To calculate the equilibrium composition of the system, the Gibbs reactor (RGIBBS) block, which is a simplified reactor model based on the minimization of the Gibbs free energy method, thus not requiring reaction stoichiometry information, was utilized. It was also assumed that the residence time inside the reactor is long enough for all the chemical reactions occurring to reach equilibrium. The chemical compounds present in the system at equilibrium were defined according to the reactions present in Table 2.1. The compounds common to all the simulations are H_2, CO, CO_2, H_2O, CH_4 and carbon, as well as smaller hydrocarbons (C_2H_6 to C_4H_{10}) and oxygenated compounds (CH_4O to $C_4H_{10}O$) that can occur due to reaction (2.4), yet, these small hydrocarbons and oxygenated compounds were not found at equilibrium in the simulations.

There are cases where using only a RGIBBS block is not enough to perform the simulation, like the simulations for reactor configurations with a hydrogen permeable membrane. To simulate the in-situ H_2 removal, a sequential modular approach is employed, as demonstrated in Figure 3.1. The MR or SEMR are divided into several (N+1) sub-reformers (represented as R in the Figure) and (N) membrane sub-separators (represented as SEP). The latter is a block that allows to separate chemical compounds according to a defined split fraction or flow (herein called hydrogen removal or recovery fraction). This split fraction is in practice related to membrane factors like its selectivity, permeability, thickness, area and process conditions (e.g. temperature, sweep-gas flow or pressure across the membrane).

In order to assess the performance for a given set of conditions employed in the simulations, the yield of the species at equilibrium must be calculated, as well as the dry-basis purity. This can be achieved resorting to the equations bellow:

$$Yield_i = \frac{m_{i,out} + \sum_{k=1}^{n} m_{i,k}}{m_{bio-oil(feed)}} \tag{3.14}$$

$$purity_{i_{,dry-basis}}(\%) = \frac{m_{i,out}}{(\sum_{i=1}^{N} m_{i,out}) - m_{H_2O,out}} x100 \quad (3.15)$$

$m_{bio-oil(feed)}$ being the molar flow rate of bio-oil in the feed of the R1 unit (1 kmol/h throughout all the simulations), $m_{i,out}$ the molar flow rate of species *i* in the outlet stream of the (RN+1) RGIBBS unit, $m_{H_2O,out}$ the molar flow rate of water in the same outlet stream and $\sum_{k=1}^{n} m_{i,k}$ the sum of the molar flow of each chemical species in the N sub-separators. This sum will always be equal to zero, except for hydrogen in the MR and the SEMR since the N sub-separators act as H_2 perm-selective membranes (with infinite selectivity towards H_2). The separation factor (fH_2) is defined as shown in Eq. (3.16):

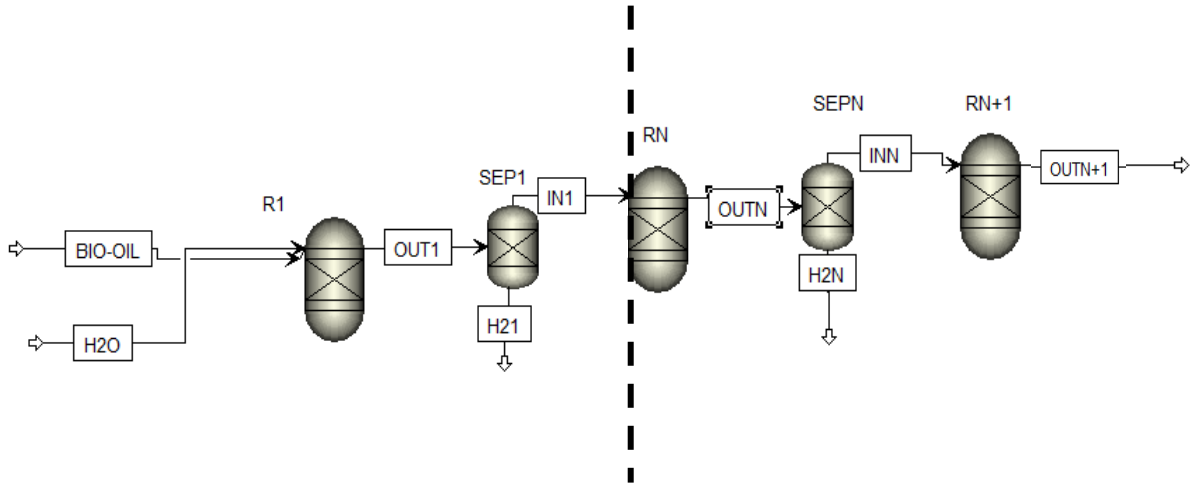

Figure 3.1 – Diagram of modular approach for simulation of a MR or SEMR.

$$fH_2 = \frac{\sum_{k=1}^{N} m_{H_2,k}}{\sum_{k=1}^{N} m_{H_2,k} + m_{H_2,N+1}} \quad (3.16)$$

where k represents each sub-separator, $\sum_{k=1}^{N} m_{H_2,k}$ represents the sum of the hydrogen molar flow rate in the permeate stream of each sup-separator and $m_{H_2,N+1}$ the hydrogen molar flow rate in the last sub-reformer.

The number of sub-separators needed in the simulation depends on the separation factor set. The higher the simulation factor, the more sub-separators will need to operate. This methodology has been implemented in previous studies [14, 27, 30, 36]. To set the separation factor in the simulation, a *design spec* needs to be created, where Eq. (3.16) is introduced in *Fortran* and the independent variable (fraction of hydrogen in the k sub-separator that is

permeated) is defined. When running the simulation, Aspen iterates the values of the independent variable in order to achieve the specified separation factor.

To simulate the sorption-enhanced reactor for CO_2 capture, three more components need to be defined, namely the sorbent (CaO was considered for the reasons mentioned before), and the products resulting from the adsorption reactions: calcium hydroxide ($Ca(OH)_2$) and calcium carbonate ($CaCO_3$) – cf. Table 2.2). Calcium oxide is then added as an inlet stream to the RGIBBS unit. The CaO to feed molar ratio can be varied in order to find the optimal value in terms of hydrogen yield and total CO_2 capture. In the simulation environment, numerous parameters can be defined such as temperature, pressure as well as the feed streams composition and molar flow rate. In this work, different bio-oil feeds were studied, and their composition varied according to their respective sources. The tables comprising the information for each bio-oil can be found in Appendix B.

For the non-stoichiometric approach herein used, it is necessary define the chemical species present in the bio-oils, however some of them do not exist in Aspen's database. In order to define them, their chemical structure was drawn and then their chemical and physical properties were obtained resorting to Aspen's estimation tool.

Lastly, to simulate the variations of temperature, water to feed molar ratio and sorbent to feed molar ratio, the Sensibility Analysis Tool from Aspen was employed, where the analysed variable and its range of variation should be introduced.

4 Results and discussion

4.1 Comparison of different bio-oils in a conventional steam reforming reactor

As it was previously stated, bio-oil originates from the pyrolysis of biomass and can come from a large array of sources. Thus, depending on the composition of the original biomass, the bio-oil derived from biomass pyrolysis will have different oxygenated compounds (see Appendix B). In this section, several bio-oils were used as feedstock, for steam reforming process, in order to compare the equilibrium yield of the products, varying either the water to feed molar ratio (WFR) or the temperature. Pressure was not varied for the conventional reactor as previous studies demonstrated that it hinders H_2 yield [27].

Through the overall steam reforming equation (2.3) it was also possible to estimate the stoichiometric WFR and the maximum H_2 yield (assuming that no parallel reactions occur), and these values can be found in Table 4.1.

Table 4.1 – Stoichiometric water to feed molar ratio (WFR) and Maximum H_2 yield for different bio-oils.

Original Biomass	Stoichiometric WFR*	Maximum H_2 Yield
Spruce wood	3	4.75
Sugar Bagasse	3	4.66
Rice husk	7	8.36
Maize stalk	7	9.53
Pine sawdust	6	8.73
Mesquite sawdust	7	9.92
Wheat shell	9	11.94
Oil palm shells	8	10.35
Oak	2	3.71
Maple	2	3.76
Eucalyptus wood	5	7.94

* Rounded up values

For all simulations carried out, the presence of the hydrocarbons and oxygenated compounds from the feed were not observed at equilibrium, meaning there is total conversion, even bellow stoichiometric WFR (not only because of the steam reforming process itself, but also due to the thermal degradation of the chemical compounds present in the feed – cf. Eq. 2.4). For that reason, results will be reported in terms of yields of produced species.

4.1.1 Effect of water to feed molar ratio

Firstly, it was studied the behaviour of the bio-oils steam reforming with a variation of the WFR (Figure 4.1). In order to compare the results obtained for a conventional reactor with those obtained for a membrane reactor and a sorption-enhanced (membrane) reactor (in the next sections), a temperature compatible with a perm-selective membrane should be established. Therefore, a temperature of 400 ºC was chosen since the Pd-Ag membrane and CaO sorbent operate in a range of 300 – 550 ºC.

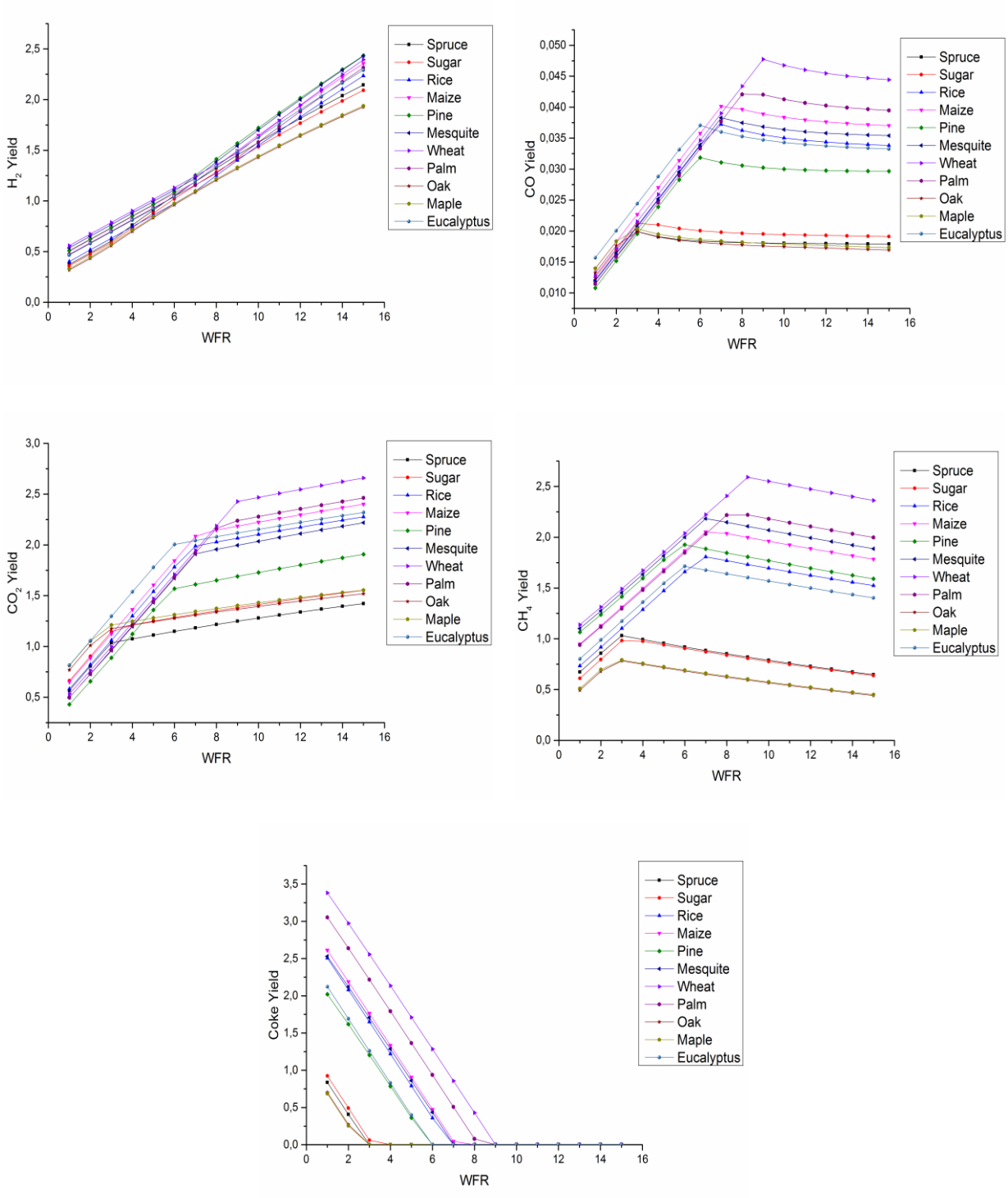

Figure 4.1 - Effect of water to feed molar ratio (WFR) on the yield of the products for several bio-oils in a steam reforming conventional reactor at 400 ºC and 1 atm.

In Figure 4.1, it is visible that all the bio-oils exhibit a similar behaviour. The H_2 yield increases with the WFR, as it shifts the equilibrium of the methane steam reforming reaction towards the conversion into hydrogen (Eq. 2.6). The excess of water also causes a slight decrease in methane production after the stoichiometric value as it will promote methane steam reforming while inhibiting methanation (Eq. 2.5). Carbon monoxide has a similar behaviour to CH_4 as it

decreases slightly when reaching the stoichiometric value, due to the fact of being consumed in the WGS reaction (Eq. 2.2), although only minor amounts of CO are present when compared to the other products. Carbon dioxide experiences a slight increase also due to the WGS reaction. Lastly, coke production is inhibited with excess water as can be perceived by the carbon formation reactions (2.10) and (2.11), thus there is no coke above the stoichiometric value.

Figure 4.1 also shows that hydrogen yields are far from the theoretical (maximum) yields predicted, as reported in Table 4.1. In order to better compare the performance of the different bio-oils, the variation of H_2 yield/maximum H_2 yield ratio with the normalized WFR (related to the stoichiometric WFR) was plotted, as can be observed in Figure 4.2. It is possible to observe that the higher the WFR/WFR_{sq} ratio is, the higher is the normalized hydrogen yield difference between the different bio-oils used. Rice has the highest yield ratio and oak has the lowest, although this is not directly connected to their maximum yield possible. While for low values they exhibit a very similar behaviour, it is possible to observe that even when the WFR is twice the WFR_{sq}, H_2 yield is still far from the maximum yield possible; this shows that there is room for improvement, either changing the reaction conditions or the reactor configuration.

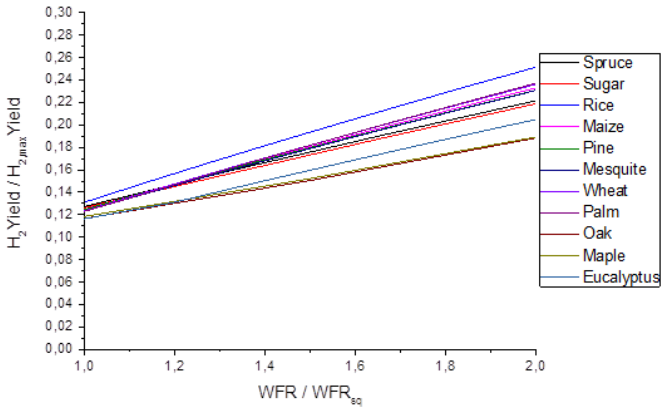

Figure 4.2 – Normalized H_2 yield as a function of the normalized water to feed molar ratio for several bio-oils at 400 °C and 1 atm.

4.1.2 Effect of temperature

The thermodynamic analysis of the temperature effect on the products yield was carried out for the different bio-oils at the stoichiometric WFR of each of them. The results can be observed in Figure 4.3.

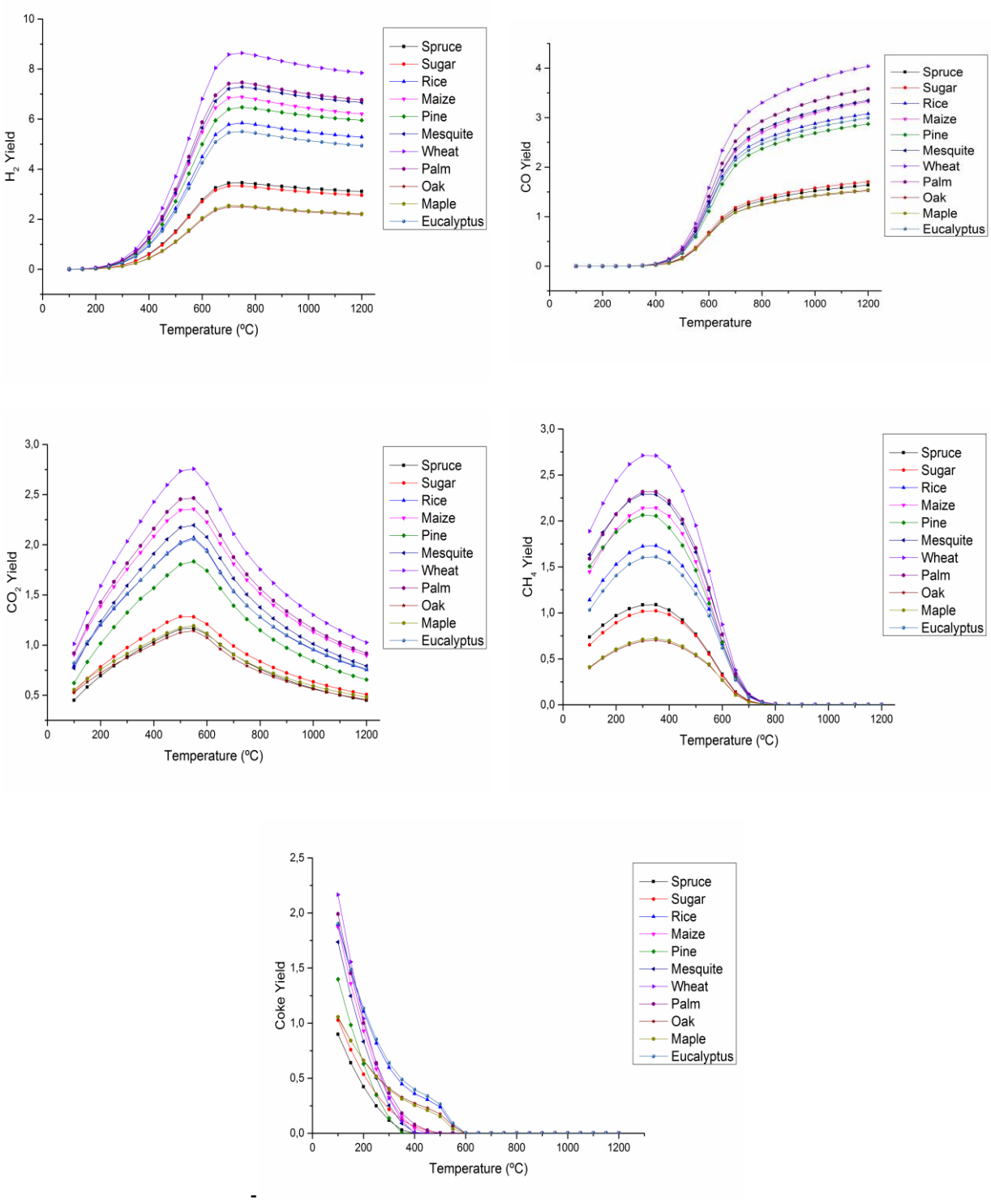

Figure 4.3 - Effect of temperature on the yield of the products for several bio-oils in a steam reforming conventional reactor at stoichiometric WFR conditions and 1 atm.

Once again, it is visible that the bio-oils exhibit similar behaviour with the increase of the temperature. Increasing temperature promotes the formation of more hydrogen due to the progressive inhibition of the methanation reaction which is highly exothermic (Eq. (2.5)); this happens until a maximum around 700 ºC and then the hydrogen yield decreases. This maximum occurs because the WGS is slightly exothermic and for temperatures above 700 ºC, reverse water-

gas shift (RWGS) is favoured. Carbon dioxide has a similar behaviour to hydrogen, but its maximum happens at lower temperatures. This happens because while H_2 is being consumed through RWGS and saved through the inhibition of methanation (the maximum yield of H_2 matches with the almost complete inhibition of methane formation), CO_2 is only being consumed through RWGS. Carbon monoxide experiences an increase from around 500ºC, since higher temperatures favour the formation of this product, either through the RWGS reactions or the inhibition of methanation. As it was already stated, for high temperatures the methanation reaction is inhibited, so there is no formation of CH_4. Besides that, for high temperatures, coke formation also does not occur as most carbon formation reactions are exothermic.

In order to better access the comparisons between the different bio-oils the normalized H_2 yield was also represented as a function of the temperature. The representation is shown in Figure 4.4 where it can also be seen that the different bio-oil behave in a similar way.

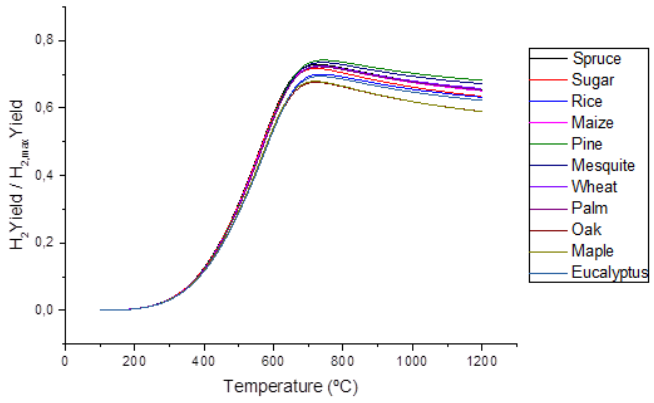

Figure 4.4 - Normalized H_2 yield as a function of temperature for several bio-oils at stoichiometric WFR and 1 atm.

Since the bio-oils have similar behaviours, for the sorption-enhanced and membrane reactors thermodynamic analysis, only two of them were chosen. The bio-oils chosen were the one from wheat shell, as it has the most H_2 production potential (see Table 4.1) and the one from spruce wood, as it is one with the lowest H_2 production potential and is a natural resource used in Portugal. The other bio-oils were assumed to have a performance in between these two.

4.2 Sorption-enhanced reactor (SER)

The objective of the SER is to remove CO_2 from the reaction zone using CaO as a CO_2 sorbent (see Eqs. 2.12-2.13), which will allow to shift the equilibrium of the steam-reforming reaction, enhancing the production of H_2.

The thermodynamic analysis was done varying the temperature and the water to feed molar ratio for different sorbent to feed molar ratios (SFR) for bio-oil derived of the pyrolysis of spruce (Figure 4.5) and wheat (Figure 4.6).

For a given temperature (in the range of 100 ºC to 700 ºC) H_2 yield rises with the SFR until reaching a maximum and then remains constant; this happens at SFR=2 for spruce and at SFR=5 for wheat as can be seen in Figures 4.5 and 4.6, respectively. This happens because the sorption reaction needs H_2O to occur (Eq. 2.12) and for the stoichiometric WFR of bio-oil steam reforming there is no enough water to make the sorption reaction fully happen, leaving unreacted CaO in the reaction zone. With the increase of the SFR for a given temperature, the CO_2 yield decreases as it would be expected, in the temperature range in which the sorption reaction operates (until 750-800 ºC), reaching zero at SFR=2 for spruce and SFR=3 for wheat (i.e. complete CO_2 sorption). The removal of CO_2 promotes the methane steam reforming (Eq. 2.6), and consequently for higher sorbent ratios it is observed a drop in CH_4 yield (in the range of 600 ºC to 800 ºC) (Figures C.1 and C.2 in Appendix). The optimum values obtained varying the temperatures for SFR=2 were 3.87 (mol H_2/mol of bio-oil) in the case of spruce, and for SFR=5 the maximum yield was 10.17 (mol H_2/mol of bio-oil) in the case of wheat, both at 450 ºC. It also peaks around this temperature, due to the sorption reaction being exothermic. Analysing the whole range of temperatures, it is worth mentioning that the removal of CO_2 shifts the WGS to produce more H_2, thus consuming CO; therefore, for low temperatures (between 100 and 600 ºC) this product is nearly inexistent as can be seen in Figures C.1 and C.2. With the temperature increase, adsorption is inhibited because the sorption reaction is exothermic and RWGS becomes more favoured, so CO formation increases. CO_2 increases with the increase of temperature until it reaches a maximum (at ca. 600 ºC), then decreases due to the inhibition of the sorption reaction and the promotion of RWGS; when there is no CaO (conventional reactor – SFR=0) this maximum is reached earlier, since only RWGS happens and not the sorption reaction(s). Lastly, due to the reduction of CO and the removal of CO_2, coke formation only occurs at very low temperatures with low SFR, as its formation depends on these two compounds (Eqs. 2.8-2.11).

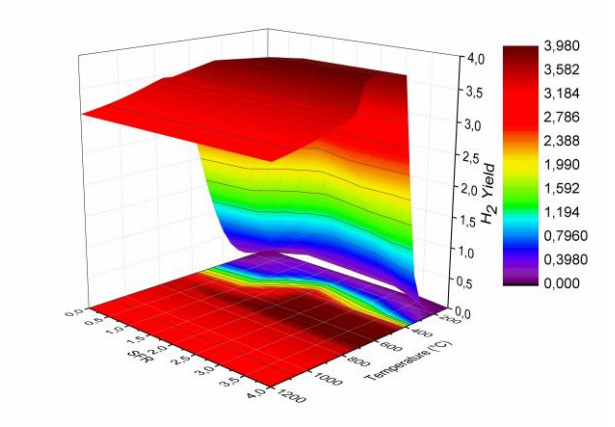

Figure 4.5 – Hydrogen yield as a function of temperature and SFR for spruce bio-oil at stoichiometric WFR and 1 atm.

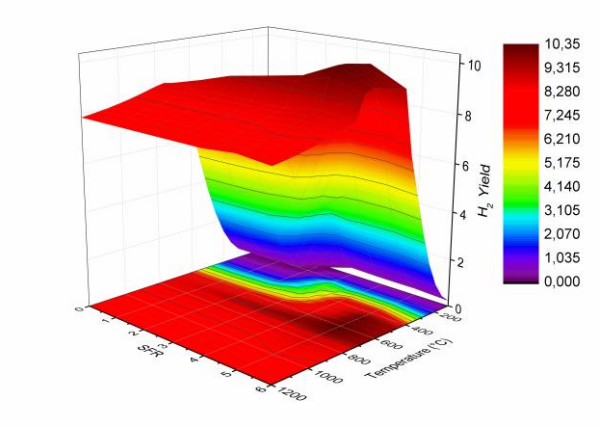

Figure 4.6 – Hydrogen yield as a function of temperature and SFR for wheat bio-oil at stoichiometric WFR and 1 atm.

For the sorption-enhanced reactor, the H_2 yield increases with the WFR (Figures 4.7 and 4.8) as it favours the methane steam reforming, WGS and also the sorption reaction(s), while inhibiting the methanation (see reactions in Tables 2.1 and 2.2); It also allows a higher CO_2 removal, and consequently for high SFR values CO_2 is inexistent (Figures C3 and C4 in Appendix C). CO has a very similar behaviour to that observed for the conventional steam reforming reactor, decreasing slightly after it reaches the stoichiometric WFR; moreover, for higher SFRs there is no carbon monoxide, because the CO_2 removal promotes the WGS reaction to completion. The increase in the water to feed molar ratio inhibits the methanation while the removal of CO_2 promotes the WGS (consuming CO); therefore, the latter indirectly contributes to the inhibition of methanation. Thus, for high values of SFR and WFR methane is not present (Figures C.3 and C.4 in Appendix C). Since both the increase of SFR and WFR inhibit the formation of coke, this compound only exists for low values of these two variables. The hydrogen yield will keep increasing with the increase of WFR until it almost reaches the theoretical maximum. In the range simulated the best value obtained was 4.71 moles for spruce at SFR= 3 and WFR=15 and 11.32 moles for wheat at SFR=5 and WFR=20. These values are respectively only 99 % and 95% from the theoretical maxim reported in Table 4.1.

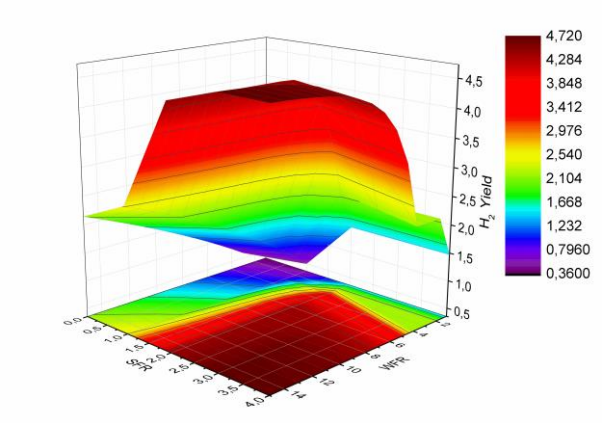

Figure 4.7 – Hydrogen yield as a function of WFR and SFR for spruce bio-oil at 400 ºC and 1 atm.

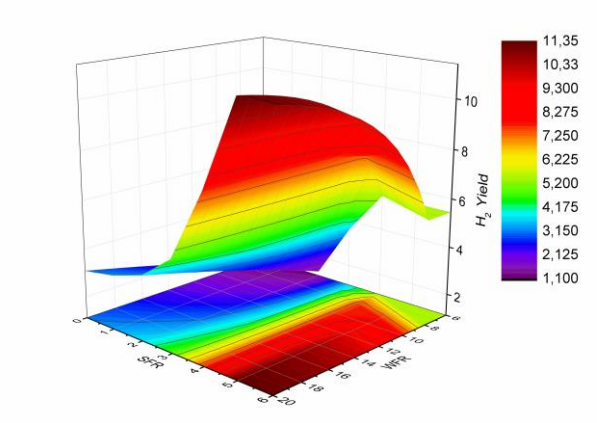

Figure 4.8 – Hydrogen yield as a function of WFR and SFR for wheat bio-oil at 400 ºC and 1 atm.

4.3 Membrane reactor (MR)

The employment of a hydrogen selective membrane in the reactor is expected to improve the hydrogen yield. The simulation for the MR was carried out analysing the behaviour of the bio-oils, varying the temperature (Figures 4.9 and 4.10) and water to feed ratio (Figures 4.11 and 4.12) for different hydrogen removal fractions. A removal fraction superior to that of 0.8 was not simulated since it is not expected to be experimentally feasible; moreover, the temperature range used was between 300 ºC and 500 ºC due to the membrane limitations.

As it was expected, with the increase of the hydrogen removal fraction, for a given temperature, the hydrogen yield increases because it inhibits the methanation, which consumes hydrogen (Eq. 2.5) and it will shift the WGS reaction to the hydrogen production side – Eq. 2.2 (see Figures 4.9 and 4.10, and specifically the projections in the bottom plane). This increase also happens with the increase of temperature, in the range used. It is noteworthy that it is possible to obtain a high hydrogen yield for lower temperatures when using the MR compared to a conventional reactor. Actually, the maximum value occurred for fH_2=0.8 at 500ºC and stoichiometric WFR was 3.44 (mol of H_2 / mol of bio-oil) for spruce and 9.31(mol of H_2 / mol of bio-oil) for wheat. As stated above, with the removal of hydrogen the methanation reaction is inhibited. Therefore, CO will be saved with the increase of temperature CO formation increases due to the RWGS (Figures C.5 and C.6 in Appendix C). Likewise, because of the inhibition of methanation, for high removal fractions of H_2 the CH_4 yield decreases. CO_2 shows the same behaviour of hydrogen, because with the inhibition of methanation the latter compound is mostly dependent of the WGS reaction. Inherently, the increase of the yield of CO_2 and CO for higher H_2

removal fractions will allow for a higher coke yield, since they are reagents in the coke formation reactions (Eqs. 2.8, 2.10 and 2.11). Because the coke formation reactions are exothermic, its formation is reduced for high temperatures (around 420 °C).

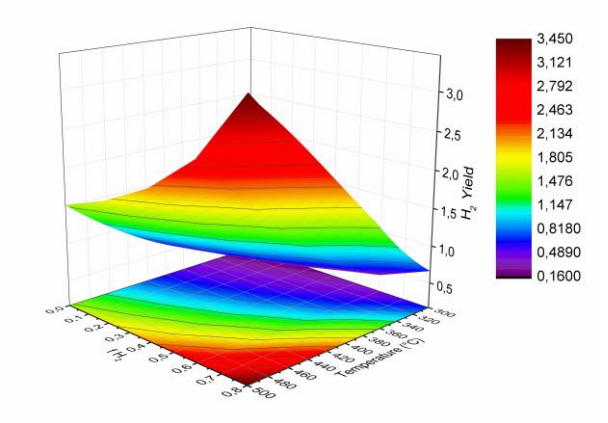

Figure 4.9 – Hydrogen yield as a function of temperature and hydrogen removal fraction for spruce bio-oil at stoichiometric WFR and 1 atm.

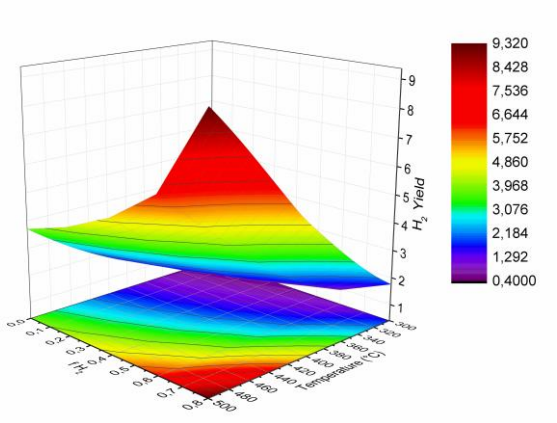

Figure 4.10 – Hydrogen yield as a function of temperature and hydrogen removal fraction for wheat bio-oil at stoichiometric WFR and 1 atm.

The increase of both the H_2 removal fraction and water to feed molar ratios promote the improvement of the hydrogen yield (Figures 4.11 and 4.12). WFR increase, beyond WFR stoichiometric where coke is not formed, promotes WGS reaction (increasing H_2 and CO_2 yield) and inhibits methanation reaction which leads to a decrease in CO yield for the same fH_2 lines. For high WFR and fH_2 values, the CO yield has an abrupt decrease in the case of spruce wood bio-oil; however, this is not verified for the wheat bio-oil, this happens because even though methanation is inhibited for these values as can be seen in the CH_4 graph (Figures C.7 and C.8 in Appendix C), the WGS reaction is still occurring thus creating that accentuated CO consumption (Figures C.7 and C.8). Carbon dioxide is affected by the same reactions as hydrogen, so it will have a similar behavior. The increase of both WFR and fH_2 inhibits methanation; so, CH_4 yield decreases with the increase of these variables. Coke formation increases with the removal fraction of hydrogen, yet it decreases with the WFR, so that for WFR values higher than 4 for spruce and 11 for wheat, coke formation does not occur.

In this reactor configuration, both for the temperatures and WFR ranges tested, H_2 is still increasing, not reaching the maximum theoretical values (Table 4.1). The best values obtained for H_2 yield were 4.66 for spruce at WFR=15 and 8.83 for wheat at WFR=20, all with a removal fraction of 0.8.

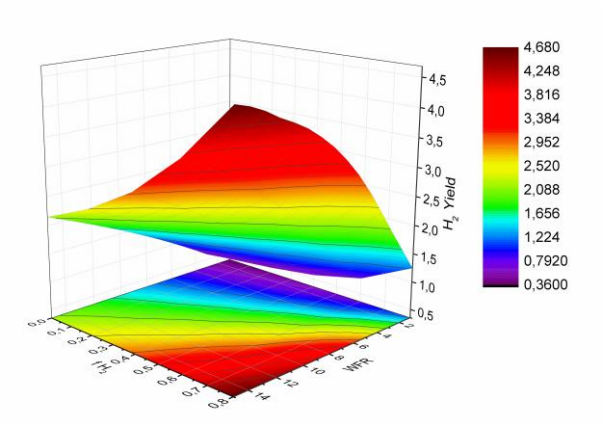

Figure 4.11 – Hydrogen yield in function of WFR and hydrogen removal fraction for spruce bio-oil at 400 ºC and 1 atm.

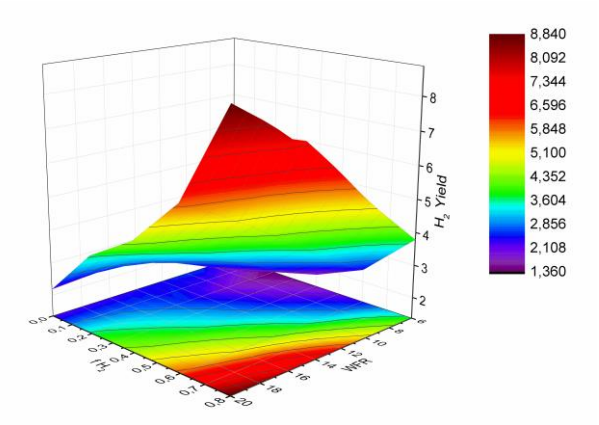

Figure 4.12 – Hydrogen yield in function of WFR and hydrogen removal fraction for wheat bio-oil at 400 ºC and 1 atm.

4.4 Sorption-enhanced membrane reactor (SEMR)

This hybrid multifunctional reactor configuration combines both carbon dioxide and hydrogen in-situ removal, which can further improve the hydrogen yield. In order to compare with previous reactor configurations, the H_2 yield is represented for the optimal values (highest H_2 yield) of each reactor configuration, which were as follows: for the SER, a SFR of 2 and 5 for bio-oil derived from spruce and wheat respectively; for the MR, a hydrogen removal fraction of 0.8; a combination of these two parameters was optimal for the SEMR. This comparison was conducted with variations of the temperature (Figures 4.13 and 4.14) and water to feed molar ratio (Figures 4.19 and 4.20). The purity of hydrogen in the outlet stream (in retentate side in the case of MR and SEMR) as a function of temperature and WFR was also determined and compared between the different reactor configurations.

Regarding the effect of temperature, the simulations were run for the respective stoichiometric WFR of each stream. It is visible from Figures 4.13 and 4.14 that for the SEMR it is possible to achieve the maximum hydrogen yield (although below the theoretical maximum) at 360 °C for spruce and at 420 °C for wheat, while for the other reactor configurations the maximum H_2 yield (always below than that for the SEMR) is achieved at a superior temperature. It is also noteworthy that the removal of CO_2 (given by SFR) has a more significant effect in the hydrogen yield improvement than the removal of H_2 (f_{H2}=0.8). Also, when capture of carbon dioxide occurs,

there is a very significant reduction of the other by-products like CO, CO_2 and coke. Methanation is also almost fully inhibited in the SEMR (Figures C.9 and C.10).

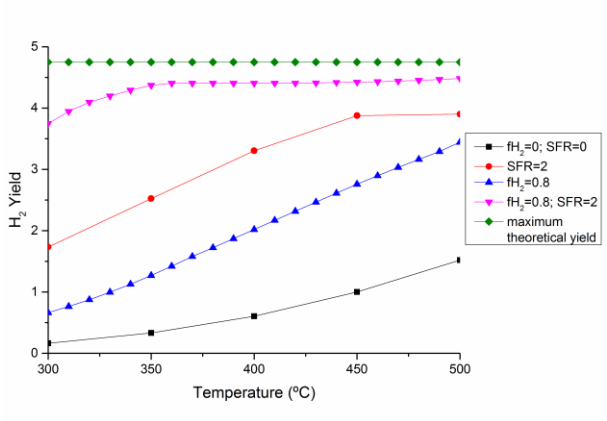

Figure 4.13 – Comparison of hydrogen yield as a function of temperature for spruce bio-oil in different reactor configurations at stoichiometric WFR and 1 atm.

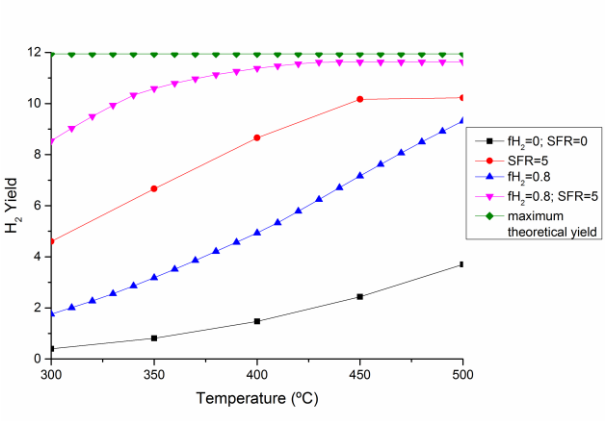

Figure 4.14 – Comparison of hydrogen yield as a function of temperature for wheat bio-oil in different reactor configurations at stoichiometric WFR and 1 atm.

Regarding H_2 purity, the effect of temperature can be observed in Figures 4.15 and 4.16. For all the reactors studied, the increase of temperature promotes a higher hydrogen purity in the retentate stream, yet for the SEMR whose feed is the bio-oil derived from pyrolysis of spruce a decrease (at ca. 400ºC) is observed. The maximum obtained purity is 95% for spruce at 450 °C in the sorption-enhanced reactor and 97% for wheat at 440 °C in the SEMR.

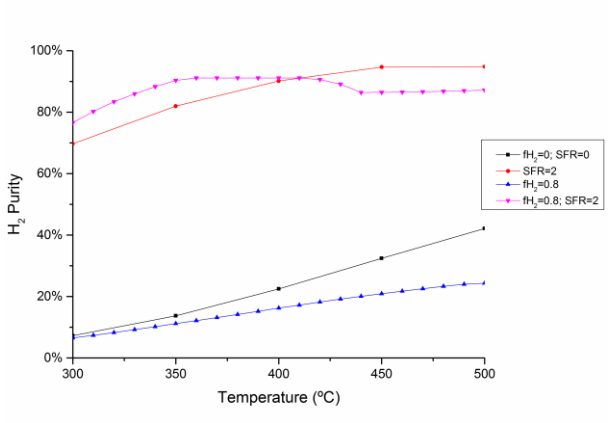

Figure 4.15 – Comparison of hydrogen purity as a function of temperature for spruce bio-oil in different reactor configurations at stoichiometric WFR and 1 atm.

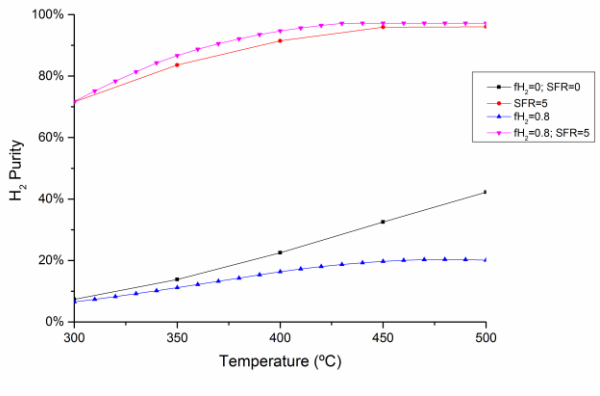

Figure 4.16 – Comparison of hydrogen purity as a function of temperature for wheat bio-oil in different reactor configurations at stoichiometric WFR and 1 atm.

To further compare the reactor configurations studied and to demonstrate how the performance is improved with the use of the hybrid reactors, the hydrogen yield was plotted at SEMR optimal temperature conditions for the different reactor configurations (Figures 4.17 and 4.18). It is visible that all reactor configurations improve the performance as compared to the conventional reactor and the best configuration is clearly the SEMR. It is noteworthy that at these conditions in the MR coke formation occurs, and consequently the SER achieves better results than the MR.

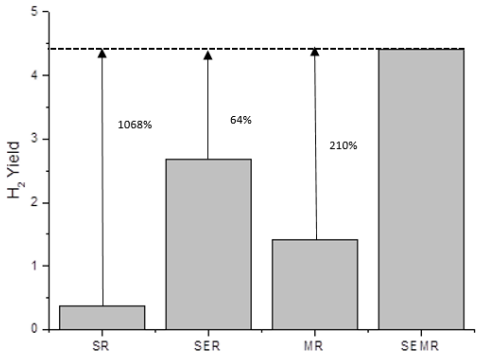

Figure 4.17 – Comparison of hydrogen yield as a function of the reactor configurations for spruce bio-oil at 360 °C, stoichiometric WFR and 1 atm.

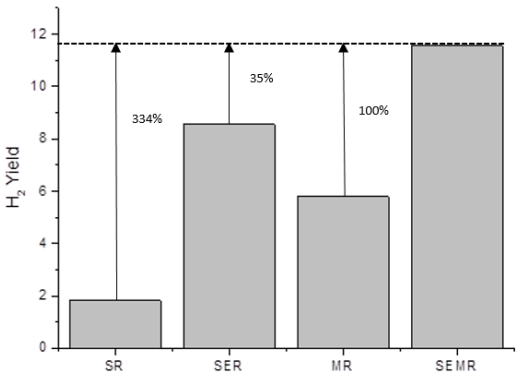

Figure 4.18 – Comparison of hydrogen yield as a function of the reactor configurations for wheat bio-oil at 420 °C, stoichiometric WFR and 1 atm.

Concerning the water to feed molar ratio, the simulations were run at 400 °C. As it has been previously stated, the increase of the WFR increases the hydrogen yield; the maximum yield was achieved at a WFR of 6 for spruce bio-oil (stoichiometric WFR =3) and 10 for wheat bio-oil (stoichiometric WFR =9) for the SEMR configuration, which is the only reactor unit able to achieve the maximum H_2 yield possible for spruce bio-oil (Figure 4.19), this is not verified for wheat bio-oil (Figure 4.20) has methanation is still occurring. The increase of steam promotes the WGS, whereas methanation is inhibited, and so the only by-product whose formation increases is carbon dioxide, which will be removed in the reactor configurations with CO_2 sorption. While carbon monoxide, methane and coke are reduced (Figures C.11 and C.12).

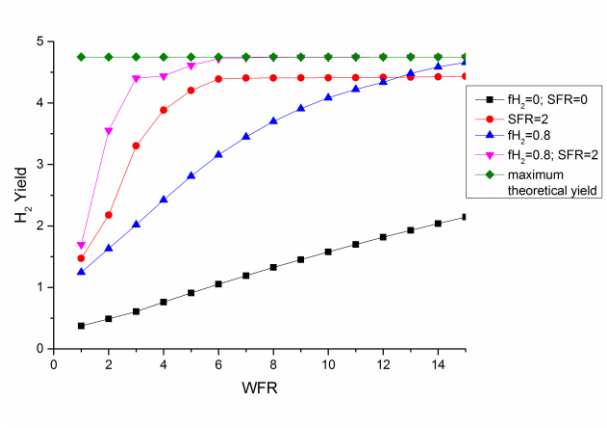

Figure 4.19 – Comparison of hydrogen yield as a function of the water to feed molar ratio (WFR) for spruce bio-oil in different reactor configurations at 400 ºC and 1 atm.

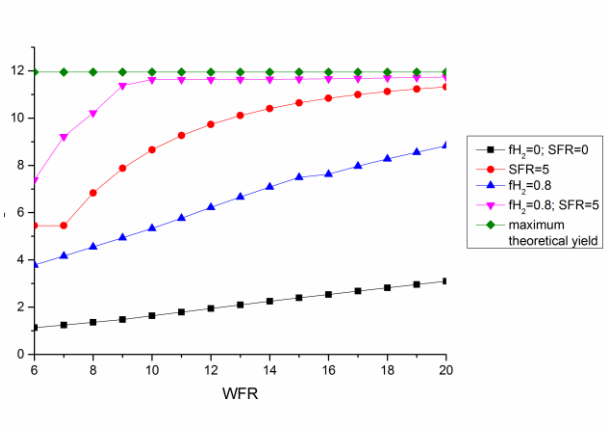

Figure 4.20 – Comparison of hydrogen yield as function of the water to feed molar ratio (WFR) for wheat bio-oil in different reactor configurations at 400 ºC and 1 atm.

With the increase of the water to feed molar ratio, the H_2 purity increases for all reactor configurations for the wheat bio-oil. However, for the spruce bio-oil steam reforming in the MR and SEMR, it increases reaching a maximum and then decreases. This happens because there is a slight increase in the yields of both CO and CO_2 (Figure C.11). The maximum purity achieved was 98% for spruce with a WFR of 6 in the sorption-enhanced configuration and 97% for wheat bio-oil with a WFR of 9 in the sorption-enhanced membrane reactor. We should recall that these purities are referred to the retentate side, being the permeate stream (for the MR and SEMR) composed by hydrogen only (because an infinitively selective membrane towards H_2 was considered to be used).

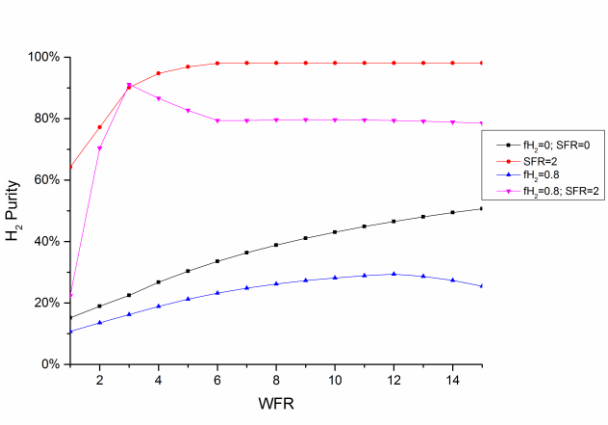

Figure 4.21 – Comparison of hydrogen purity as a function of WFR for spruce bio-oil for different reactor configurations at 400 ºC and 1 atm.

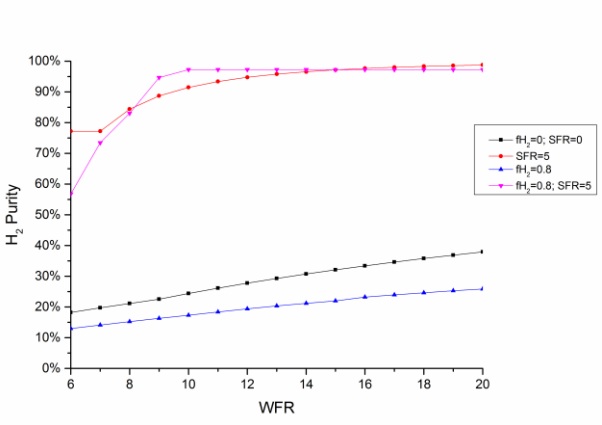

Figure 4.22 – Comparison of hydrogen purity as a function of WFR for wheat bio-oil for different reactor configurations at 400 ºC and 1 atm.

The comparison between the reactor configurations at WFR optimal conditions for SEMR was also performed (Figures 4.23 and 4.24). The conclusions obtained are equal to those of the comparison at optimal temperature conditions. Once again, with this WFR, MR will still have coke formation which leads to lower H_2 yield as compared to either the SER or SEMR.

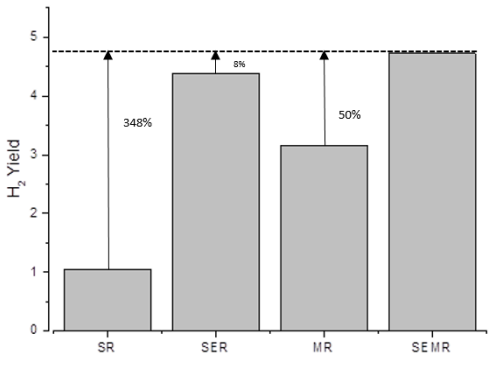

Figure 4.23 – Comparison of hydrogen yield in function of reactor configurations for spruce bio-oil at 400 °C, WFR=6 and 1 atm.

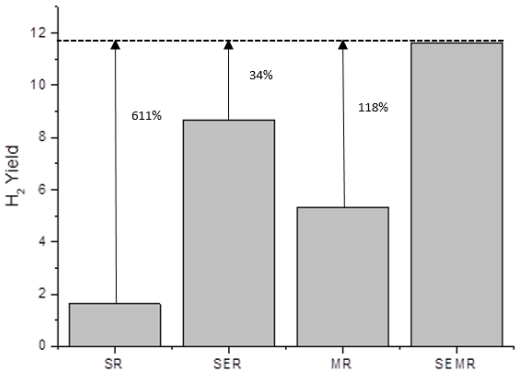

Figure 4.24 – Comparison of hydrogen yield in function of reactor configurations for wheat bio-oil at 400 °C, WFR=10 and 1 atm.

4.5 Effect of pressure

As stated above, pressures higher than 1 bar will shift the thermodynamic equilibrium to the reagents side, detrimentally affecting the hydrogen yield. However, the pressure favours the CO_2

sorption capacity of the sorbent and the driving force for H_2 permeation through a H_2 perm-selective membrane [34]. Therefore, when working with membranes it is not realistic to expect to achieve hydrogen removal fractions as high as 0.8 at 1 atm. For this reason, for the MR and SEMR pressures up to 10 bar were simulated for the situations in which these reactors showed the highest hydrogen yields, SFR and fH_2. Temperature was fixed at 400 °C and the WFR at the stoichiometric value. The results obtained are presented in Figures 4.25 and 4.26 for bio-oil derived from pyrolysis of spruce and wheat, respectively.

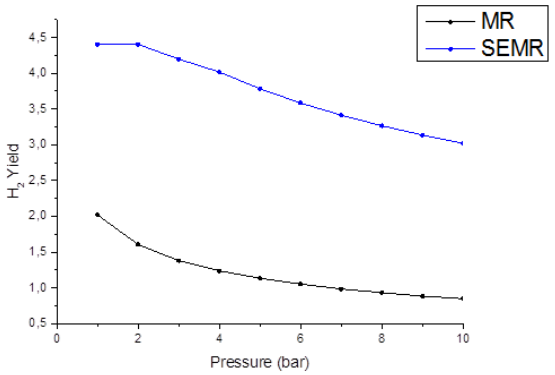

Figure 4.25 – Hydrogen yield as a function of pressure for spruce bio-oil at 400 ºC, stoichiometric WFR, $fH_2 = 0.8$ and SFR=2.

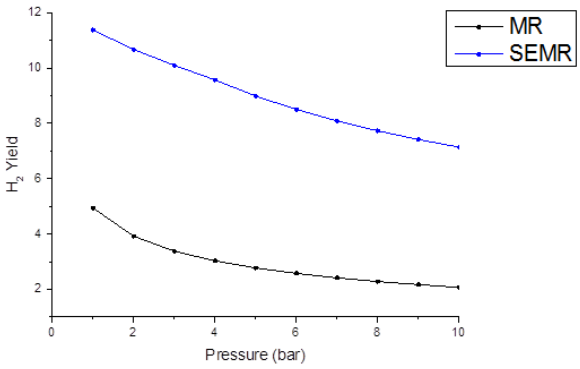

Figure 4.26 – Hydrogen yield as a function of pressure for wheat bio-oil at 400 ºC, stoichiometric WFR, $fH_2 = 0.8$ and SFR=5.

As expected, it is visible that the increase of pressure reduces the hydrogen yield. This reduction is more visible, in absolute values, in the SEMR than in the MR; yet the SEMR allows to attain a much greater H_2 yield, due to the carbon dioxide capture. It is also visible that between 1 and 2 bar, the difference in hydrogen yield is not very significant in the SEMR, especially for spruce bio-oil. The fact that this reduction is low is relevant because experimental studies already presented in Chapter 2 showed that a slight increase of pressure (from 1 bar to 1.5) may improve hydrogen yield for a membrane reactor [34]. Of course, such studies are not under equilibrium (thermodynamic) conditions and kinetics is of paramount importance.

The negative effect of pressure can be overcome by the increase of WFR. Since the conversion is complete and there is no carbon present, the yields of the products will be affected by methanation and WGS, being methanation the only reaction affected by pressure changes. The increase of WFR inhibits methanation which will lead to a more stable H_2 yield as a function of pressure [27]. This was tested for the SEMR, since it is the configuration that allows for a higher H_2 yield. The results obtained are present in Figures 4.27 and 4.28.

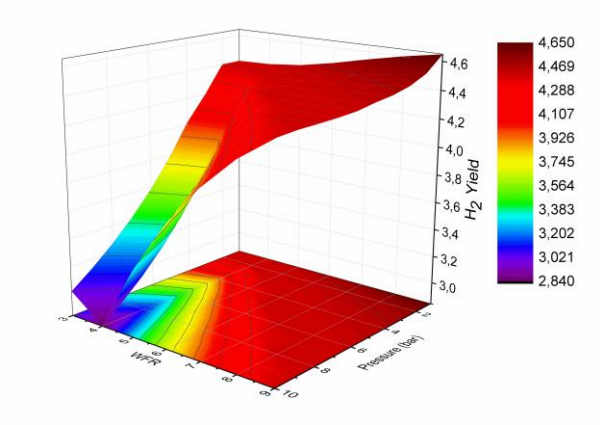

Figure 4.27 – Hydrogen yield as a function of pressure and water to feed ratio (WFR) for spruce bio-oil at 400 ºC, $fH_2 = 0.8$ and SFR=2.

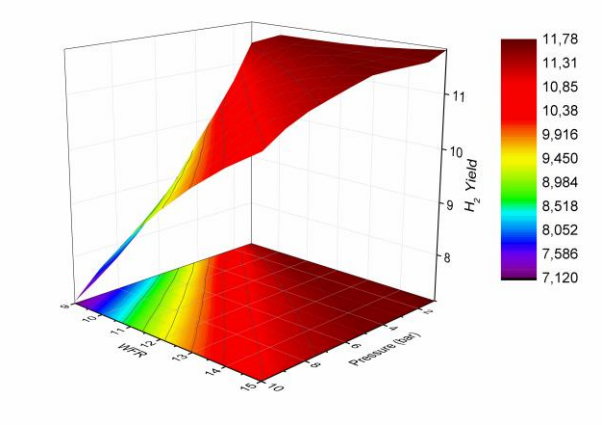

Figure 4.28 – Hydrogen yield as a function of pressure and water to feed ratio (WFR) for wheat bio-oil at 400 ºC, $fH_2 = 0.8$ and SFR=5.

It is visible that the increase of the WFR had a positive effect in the variation of the H_2 yield. While previously, at the stoichiometric WFR the H_2 yield decreased 31% for spruce and 37% for wheat when the total pressure was changed from 1 bar to 10 bar, the decrease is now only 5% for spruce at WFR=9 and 8% for wheat at SFR=15. In addition, it is worth noting that a pressure as high as 10 bar might not be needed to achieve the removal fraction of 0.8.

4.6 Energetically neutral conditions

In the steam reforming process, heat is commonly needed to maintain the reactor at the desired temperature, since the SR reaction is endothermic. Until now the energy needed was not considered, only the maximization of the hydrogen yield and the minimization of the sub-products was aimed. The feed was maintained at 400 °C and only the temperature of the reactor was varied, but in practice pre-heating the feed to this temperature has associated costs and does not ensure that energetically neutral conditions are met (when the heat duty for the reactor is null).

An alternative to heating the feed is profit from the heat released during CO_2 sorption since the sorption reactions are exothermic (cf. Table 2.2) and may generate the heat needed to maintain the reactors' temperature. The minimum SFR needed to assure energetically neutral conditions was identified for the SER and SEMR and the H_2 yield obtained for these conditions was computed. For this, the reactor temperature was kept at 500 °C and the feed temperature was varied between 150 °C and 500 °C. The results obtained are presented in Figures 4.27 and 4.28.

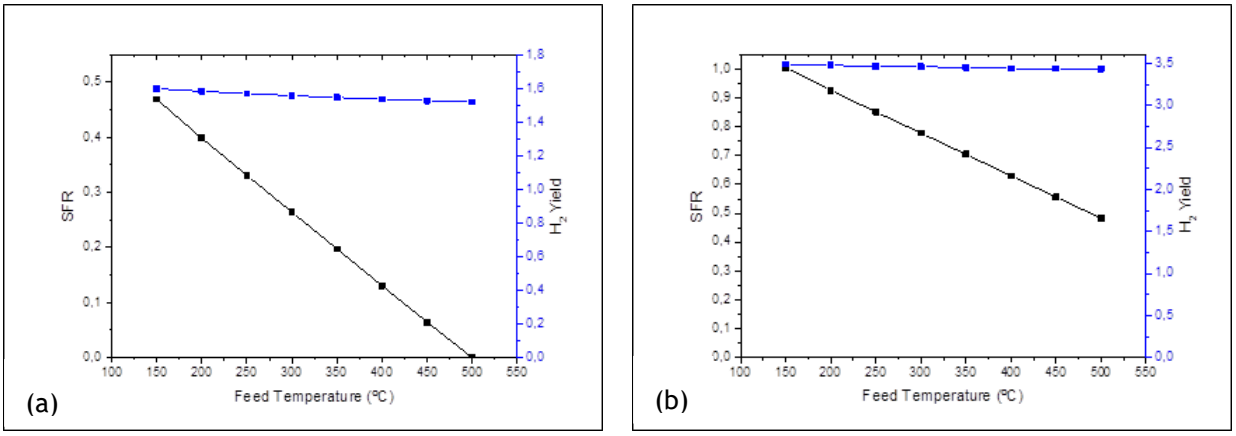

Figure 4.29 – Minimum SFR needed to achieve energetically neutral conditions and H_2 yield (blue) as a function of feed temperature (at 500 °C and stoichiometric WFR) for spruce bio-oil in a) a SER and b) SEMR with $fH_2 = 0.8$.

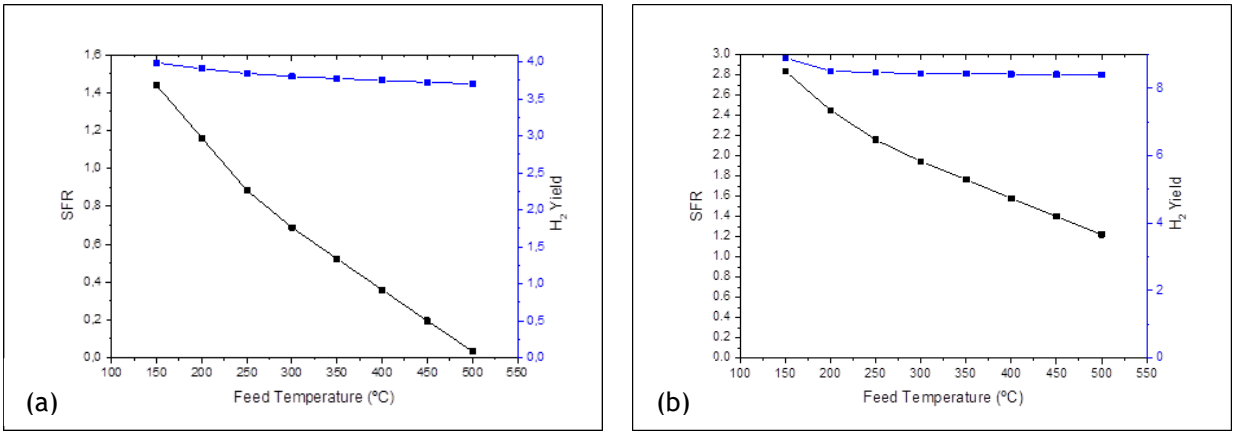

Figure 4.30 – Minimum SFR needed to achieve energetically neutral conditions and H_2 yield (blue) as function of feed temperature (at 500 °C and stoichiometric WFR) for wheat bio-oil in a) a SER and b) SEMR with $fH_2 = 0.8$.

From the analysis of these figures, it is possible to conclude that a greater amount of sorbent is needed in the SEMR, because the removal of hydrogen inhibits the exothermic methanation reaction. The higher the feed temperature, the lower will be the SFR needed to achieve energetically neutral conditions, as expected. Furthermore, the variations of these conditions causes little variation in the hydrogen yield, that decreases only slightly with the decrease of the SFR.

The SFR needed to achieve energetically neutral conditions is lower than the SFR that showed higher hydrogen yield in previous sections where the CO_2 was completely captured. This means that under energetically neutral conditions there is still CO_2 that can be captured, which would

lead to lower H_2 yield. Hence, if the SFR used in previous section (SFR=2 for spruce and SFR=5 for wheat) is employed, and since the CO_2 sorption reactions (Eqs. 2.12 and 2.13) are exothermic, there will be no need to supply heat to the reactor, but it might need cooling in order to maintain the temperature.

5 Conclusions and future work

5.1 Conclusions

A thermodynamic analysis of the species present in the chemical equilibrium of the steam reforming process for several pyrolysis bio-oils was carried out in order to access the effects of different important operating parameters on the hydrogen (and by-products) yield. This analysis was performed in different reactor configurations in order to find the best one and the operational conditions that allow to maximize the hydrogen yield.

In the case of the conventional reactor, temperature and water to feed ratio (WFR) showed a positive impact in the production of hydrogen. Comparing the steam reforming of the different bio-oils, although the hydrogen yield is superior in those that have larger quantities of more complex hydrogenated components, they showed similar behaviour with respect to variations of temperature or WFR. Due to that it was possible to choose two of them (spruce wood and wheat shell) as representatives in the simulations for the different reactor configurations that were subsequently analysed.

The in-situ CO_2 removal using calcium oxide as sorbent in a sorption-enhanced reactor (SER) and the in-situ removal of H_2 through a selective permeable membrane (membrane reactor - MR) allowed an increase of the hydrogen production while also inhibiting the formation of carbon monoxide, methane and coke, compared to a conventional reactor. Furthermore, the sorption-enhanced configuration also removes carbon dioxide from the outlet stream, allowing for an increase in the hydrogen purity (dry-basis). The MR allows to reach high hydrogen yields at lower temperatures than those employed in the conventional steam reforming reactor. Although it reduces the hydrogen purity in the outlet retentate stream, a significant part of the hydrogen is removed through the membrane (resulting in a high-purity H_2 stream in the permeate side).

On the other hand, the sorption-enhanced membrane reactor (SEMR) allows to achieve almost the maximum possible hydrogen yield at low temperatures, 4.40 H_2 mol/bio-oil mol at 360 °C for spruce wood and 11.55 H_2 mol/bio-oil mol at 420 °C for wheat shell. This performance is also achieved at the stoichiometric water to feed ratios, not needing a superior flow rate of steam. The best values reached were also obtained for this reactor configuration, 4.72 H_2 mol/bio-oil mol for spruce (at 400 °C, WFR = 6, SFR = 2, fH2 = 0.8 and 1 bar) and 11.62 H_2 mol/bio-oil mol for wheat (at 400 °C, WFR = 10, SFR = 5, fH2 = 0.8 and 1 bar). Therefore, this reactor configuration is the one that provides the best hydrogen yield from a thermodynamic stand-point.

The configurations with a hydrogen permeable selective membrane show a high H_2 yield for a hydrogen removal fraction of 0.8, which is a high value not easy to achieve at atmospheric pressure. For this reason, the effect of pressure was simulated for the MR and SEMR configuration, as an increase of pressure would ensure that high removal fractions can be achieved. Results showed that hydrogen yield decreased with pressure, yet, with the SEMR configuration the decrease was not very significant for low pressure increases and this reduction can be overcome by the increment of the WFR.

The sorption-enhanced configuration with CO2 capture shows a higher H_2 yield than that for the membrane reactor. Even though the hydrogen yield is not as elevated as the one for the sorption-enhanced membrane reactor, high values can still be achieved, namely 3.87 H_2 mol/bio-oil mol at 450 °C for spruce wood and 10.17 H_2 mol/bio-oil mol also at 450 °C for wheat shell. - Furthermore, this configuration also allows to obtain a high purity hydrogen outlet stream.

Lastly, energetically neutral conditions were simulated. These simulations showed that the sorbent to feed ratio needed to maintain these conditions was not that high (lower than the SFR that showed the best H_2 yield for both bio-oils). This shows that it might be viable to use a CO_2 sorbent to minimize the energy needed for the process instead of heating the feed.

5.2 Future work

Regarding the analysis carried out in this work, a few aspects can be targeted for future research aiming the efficient use of bio-oils to produce hydrogen. There are different sorbents that can be used for in-situ CO_2 removal at high temperatures (e.g. hydrocalcites); these could also be thermodynamically analysed to see how they would perform in the steam reforming process and how they would affect the equilibrium compositions. Furthermore, experimental tests would be important to perform and verify, by comparing with the results gathered in the simulations, how far the results are from the thermodynamic limits.

Furthermore, it would be very important to perform an economic balance to all the reactor configurations that were simulated in order to determine which one would be the more profitable and if the use of higher water to feed ratios and sorbent to feed ratios are economically sustainable. Of course, the energy spent to operate and its cost should also be contemplated in the economic balance. This economic analysis should be carried for the different bio-oils, since they present different steam needs for the reaction to occur and provide different hydrogen yields. Besides this, they also come from different sources, which implies that their cost will change, so it would be

interesting to determine which one would be more economically advantageous. This strategy could be subsequently extended to a life cycle analysis of the whole process.

6 Bibliography

1. Rojey, A., A. Minkkinen, and E. Lebas, *Combined Production of Hydrogen, Clean Power and Quality Fuels*. 2004.
2. Antunes, F., *Produção de combustíveis e de energia eléctrica a partir da Biomassa lenhocelulósica*. 2008, Universidade do Porto: Faculdade de Engenharia.
3. Turkenburg, W.C., *World Energy Assessment of the United Nations: energy and the challenge of sustainability*, D.o.E.a.S. Affairs, Editor. September 2000.: New York. p. 219-272.
4. Mondal, P., G.S. Dang, and M.O. Garg, *Syngas production through gasification and cleanup for downstream applications — Recent developments*. Fuel Processing Technology, 2011. **92**(8): p. 1395-1410.
5. Oasmaa, A. and D. Meier, *Norms and standards for fast pyrolysis liquids*. Journal of Analytical and Applied Pyrolysis, 2005. **73**(2): p. 323-334.
6. Bridgwater, T., *Biomass for energy*. Journal of the Science of Food and Agriculture, 2006. **86**(12): p. 1755-1768.
7. Raffelt K, H.E., Koegel A, Stahl R, Steinhardt J, Weirich F., *The BTL2 process of biomass utilization entrained-flow gasification of pyrolyzed biomass slurries*. Applied Biochemistry and Biotechnology, 2006. **129**(1-3): p. 153–164.
8. S. Czernik and A.V. Bridgwater, *Overview of Applications of Biomass Fast Pyrolysis Oil*. Energy & Fuels, 2004. **18**(2): p. 590-598.
9. Adhikari, S., S.D. Fernando, and A. Haryanto, *Hydrogen production from glycerol: An update*. Energy Conversion and Management, 2009. **50**(10): p. 2600-2604.
10. Energy, O.o.E.E.R. *HYDROGEN PRODUCTION: NATURAL GAS REFORMING*. [cited 2017 16 March]; Available from: https://energy.gov/eere/fuelcells/hydrogen-production-natural-gas-reforming.
11. Remiro, A., B. Valle, A.T. Aguayo, J. Bilbao, and A.G. Gayubo, *Operating conditions for attenuating Ni/La2O3-aAl2O3 catalyst deactivation in the steam reforming of bio-oil aqueous fraction*. Fuel Processing Technology, 2013. **115**: p. 222-232.
12. Montero, C., L. Oar-Arteta, A. Remiro, A. Arandia, J. Bilbao, and A.G. Gayubo, *Thermodynamic comparison between bio-oil and ethanol steam reforming*. International Journal of Hydrogen Energy, 2015. **40**(46): p. 15963-15971.
13. Goicoechea, S., H. Ehrich, P.L. Arias, and N. Kockmann, *Thermodynamic analysis of acetic acid steam reforming for hydrogen production*. Journal of Power Sources, 2015. **279**: p. 312-322.
14. Leal, A.L., M.A. Soria, and L.M. Madeira, *Autothermal reforming of impure glycerol for H2 production: Thermodynamic study including in situ CO2 and/or H2 separation*. International Journal of Hydrogen Energy, 2016. **41**(4): p. 2607-2620.
15. D. Wang, S. Czernik, D. Montane, M. Mann, and E. Chornet, *Biomass to Hydrogen via Fast Pyrolysis and Catalytic Steam Reforming of the Pyrolysis Oil or Its Fractions*. Industrial & Engineering Chemistry Research, 1997. **36**(5): p. 1507–1518.
16. Abbas, S.Z., V. Dupont, and T. Mahmud, *Kinetics study and modelling of steam methane reforming process over a NiO/Al 2 O 3 catalyst in an adiabatic packed bed reactor*. International Journal of Hydrogen Energy, 2017. **42**(5): p. 2889-2903.
17. Dinesh Mohan, C.U.P. Junior, and P.H. Steele, *Pyrolysis of Wood/Biomass for Bio-oil: A Critical Review*. Energy & Fuels, 2006. **20**(3): p. 848–889.

18. D. Wang, S. Czernik, D. Montane, M. Mann, and E. Chornet, *Biomass to Hydrogen via Fast Pyrolysis and Catalytic Steam Reforming of the Pyrolysis Oil or Its Fractions.* 1997.

19. Panagiotis N. Kechagiopoulos, Spyros S. Voutetakis, Angeliki A. Lemonidou, and I.A. Vasalos, *Hydrogen Production via Steam Reforming of the Aqueous Phase of Bio-Oil in a Fixed Bed Reactor.* Energy & Fuels, 2006. **20**(5): p. 2155–2163.

20. Chen, G., J. Tao, C. Liu, B. Yan, W. Li, and X. Li, *Hydrogen production via acetic acid steam reforming: A critical review on catalysts.* Renewable and Sustainable Energy Reviews, 2017. **79**: p. 1091-1098.

21. Trane, R., S. Dahl, M.S. Skjøth-Rasmussen, and A.D. Jensen, *Catalytic steam reforming of bio-oil.* International Journal of Hydrogen Energy, 2012. **37**(8): p. 6447-6472.

22. Alírio E. Rodrigues, Luís M. Madeira, Y.-J. Wu, and R.P.V. Faria, *Sorption Enhanced Reaction Processes.* In Press: World Scientific Publishing.

23. Avasthi, K.S., R.N. Reddy, and S. Patel, *Challenges in the Production of Hydrogen from Glycerol – A Biodiesel Byproduct Via Steam Reforming Process.* Procedia Engineering, 2013. **51**: p. 423-429.

24. Gil, M.V., J. Fermoso, C. Pevida, D. Chen, and F. Rubiera, *Production of fuel-cell grade H2 by sorption enhanced steam reforming of acetic acid as a model compound of biomass-derived bio-oil.* Applied Catalysis B: Environmental, 2016. **184**: p. 64-76.

25. Dou, B., Y. Song, C. Wang, H. Chen, and Y. Xu, *Hydrogen production from catalytic steam reforming of biodiesel byproduct glycerol: Issues and challenges.* Renewable and Sustainable Energy Reviews, 2014. **30**: p. 950-960.

26. Soria, M.A., S. Tosti, A. Mendes, and L.M. Madeira, *Enhancing the low temperature water–gas shift reaction through a hybrid sorption-enhanced membrane reactor for high-purity hydrogen production.* Fuel, 2015. **159**: p. 854-863.

27. Silva, J.M., M.A. Soria, and L.M. Madeira, *Thermodynamic analysis of Glycerol Steam Reforming for hydrogen production with in situ hydrogen and carbon dioxide separation.* Journal of Power Sources, 2015. **273**: p. 423-430.

28. Iordanidis, A., P. Kechagiopoulos, S. Voutetakis, A. Lemonidou, and I. Vasalos, *Autothermal sorption-enhanced steam reforming of bio-oil/biogas mixture and energy generation by fuel cells: Concept analysis and process simulation.* International Journal of Hydrogen Energy, 2006. **31**(8): p. 1058-1065.

29. Shigeyuki Uemiya, Noboru Sato, Hiroshi Ando, T. Matsuda, and E. Kikuchi, *Steam reforming of methane in a hydrogen-permeable membrane reactor* Applied Catalysis, 1991. **67**(1): p. 223-230.

30. Basile, A., A. Iulianelli, T. Longo, S. Liguori, and M. De Falco, *Chapter 2 - Pd-based Selective Membrane: State-of-the-Art*, in *Membrane Reactors for Hydrogen Production Processes*, Springer, Editor. 2011.

31. Shigeyuki Uemiya, T. Matsuda, and E. Kikuchi, *Hydrogen permeable palladium-silver alloy membrane supported on porous ceramics* Journal of Membrane Science, 1991. **56**(3): p. 315-325.

32. Okazaki, J., T. Ikeda, D.A.P. Tanaka, K. Sato, T.M. Suzuki, and F. Mizukami, *An investigation of thermal stability of thin palladium–silver alloy membranes for high temperature hydrogen separation.* Journal of Membrane Science, 2011. **366**(1-2): p. 212-219.

33. Wang, X., N. Wang, M. Li, S. Li, S. Wang, and X. Ma, *Hydrogen production by glycerol steam reforming with in situ hydrogen separation: A thermodynamic investigation.* International Journal of Hydrogen Energy, 2010. **35**(19): p. 10252-10256.

34. Iulianelli, A., T. Longo, and A. Basile, *CO-free hydrogen production by steam reforming of acetic acid carried out in a Pd–Ag membrane reactor: The effect of co-current and counter-current mode.* International Journal of Hydrogen Energy, 2008. **33**(15): p. 4091-4096.

35. Chen, H., T. Zhang, B. Dou, V. Dupont, P. Williams, M. Ghadiri, and Y. Ding, *Thermodynamic analyses of adsorption-enhanced steam reforming of glycerol for hydrogen production.* International Journal of Hydrogen Energy, 2009. **34**(17): p. 7208-7222.

36. Xiaodong Wang, S.L., Hao Wang, Bo Liu, and Xinbin Ma, *Thermodynamic Analysis of Glycerin Steam Reforming.* Energy & Fuels, 2008. **22**(6): p. 4285–4291.

37. Chang, S., Z. Zhao, A. Zheng, F. He, Z. Huang, and H. Li, *Characterization of Products from Torrefaction of Sprucewood and Bagasse in an Auger Reactor.* Energy & Fuels, 2012. **26**(11): p. 7009-7017.

38. Ji-lu, Z., *Bio-oil from fast pyrolysis of rice husk: Yields and related properties and improvement of the pyrolysis system.* Journal of Analytical and Applied Pyrolysis, 2007. **80**(1): p. 30-35.

39. Zheng, J.-L., *Pyrolysis oil from fast pyrolysis of maize stalk.* Journal of Analytical and Applied Pyrolysis, 2008. **83**(2): p. 205-212.

40. Bertero, M., G. de la Puente, and U. Sedran, *Fuels from bio-oils: Bio-oil production from different residual sources, characterization and thermal conditioning.* Fuel, 2012. **95**: p. 263-271.

41. !!! INVALID CITATION !!! .

42. Chang, S., Z. Zhao, A. Zheng, X. Li, X. Wang, Z. Huang, F. He, and H. Li, *Effect of hydrothermal pretreatment on properties of bio-oil produced from fast pyrolysis of eucalyptus wood in a fluidized bed reactor.* Bioresour Technol, 2013. **138**: p. 321-8.

Appendix A

The Soave-Redlich-Kwong equation of state is given by:

$$P = \frac{RT}{v-n} - \frac{a\alpha(T)}{v(v+b)} \quad (A.1)$$

$$a\alpha(T) = 0.42748\frac{r^2 T_C^2}{P_C \alpha(T)} \quad (A.2)$$

$$b = 0.08664\frac{RT}{P_C} \quad (A.3)$$

$$\alpha(T) = [1 + m(1 - T_r^{0.5})]^2 \quad (A.4)$$

$$T_r = \frac{T}{T_C} \quad (A.5)$$

$$m = 0.480 + 1.574\omega - 0.176\omega^2 \quad (A.6)$$

where P represents the gas pressure, P_C the critical pressure, R the ideal gas constant, T the temperature, T_r is the reduced temperature and T_C the critical temperature. v represents the molar volume, a is a constant that corrects for the attractive potential of molecules, b is a constant that corrects for volume and lastly, ω represents the acentric factor.

The fugacity coefficient can be calculated through equation (A.7)

$$ln\hat{\phi}_i = \frac{b_i}{b_m}(Z-1) - \frac{\ln P(v-b_m)}{RT} + \frac{a_m}{b_m RT}\left(\frac{b_i}{b_m} - \frac{2}{a_m}\sum_{k=1}^{N} y_k a_{ik}\right)\ln\left(1 + \frac{b_m}{V}\right) \quad (A.7)$$

The mixture parameters from Eq. (A.7) can be defined by the mixture rules as follows:

$$a_m = \sum_i \sum_k y_i y_k a_{ik} \quad (A.8)$$

$$b_m = \sum_i y_i b_i \quad (A.9)$$

$$a_{ik} = (a_i a_k)^{0.5}(1 - k_{ik}) \quad (A.10)$$

Appendix B

In this Appendix, the tables containing the dry-basis chemical composition of the different bio-oils are presented. Some bio-oils (pine sawdust, mesquite saw, wheat shell and eucalyptus wood) had a sizeable array of chemical species, and for that reason only compounds with a weight percentage superior to 1% were considered for the simulations. Furthermore, compounds like xylenol and cresol have 6 and 3 isomers, respectively, so when the literature does not describe in which percentage the isomers are present, an equal fraction of each isomer was considered for the simulations.

Table B.1 - Composition of spruce wood bio-oil [37].

Chemical compound	%molar
Acetic acid	43.42%
Propionic acid	0.67%
Methanol	37.28%
Acetol	10.07%
Furfural	3.36%
Furfuryl alcohol	2.50%
Phenol	0.05%
Guaiacol	0.85%
Eugenol	0.30%
Isoeugenol	0.87%
Vanillin	0.62%

Table B.2 - Composition of sugar bagasse bio-oil [37].

Chemical compound	%molar
Acetic acid	74.09%
Propionic acid	1.10%
Methanol	12.36%
Acetol	4.83%
Furfural	4.22%
Furfuril alcohol	1.86%
Phenol	0.43%
Guaiacol	0.38%
Eugenol	0.29%
Isoeugenol	0.27%
Vanillin	0.18%

Table B.3 - Composition of rice husk bio-oil [38].

Chemical compound	%molar
Formic acid	51.35%
β-Hydroxybutyric acid	6.82%
Toluene	16.68%
Benzoic acid. 3-methyl-	2.60%
Phthalic acid	2.26%
2-Cyclopentane-1-one. 3-methyl	4.54%
4H-Pyran-4-one. 2.6-dimethyl-	5.32%
Acetovanillone	1.85%
Benzaldehyde. 2-hydroxyl	4.66%
Benzaldehyde. 3.5-dimethyl-4-hydroxyl	3.93%

Table B.4 - Composition of maize stalk bio-oil [39].

Chemical compound	%molar
Dihydroxyacetone	17.83%
Acetic acid	18.52%
Propionic acid	8.90%
Butyric acid	7.01%
3-Methyl-2-cyclopenten-1-one	7.28%
1-Hydroxybutan-2-one	8.88%
Dimethyl succinate	8.17%
Phenol	6.13%
Guaiacol	8.29%
2-Acetylfuran	8.98%

Table B.5 - Composition of pine sawdust bio-oil [40].

Chemical compound	%molar
Acetic acid	11.74%
Isocrotonic acid	1.48%
Butanoic acid. 2-hydroxy-	3.18%
Pentanoic acid. 4-methyl-	5.72%
Acetic anhydride	1.73%
Methyl butanoate	2.78%
Acetone	3.68%
2-Butenal	4.02%
2-Butanone	1.80%
2-Pentanone. 1-hydroxy-	1.67%
2-Pentanone	3.18%
2.3-Pentadione	6.06%
2-Butanone. 4-hydroxy-3methyl-	1.32%
Octanal	1.62%
Cyclopentanone	1.55%
Cyclopentenone. 2-hydroxy-3-methyl-	1.46%
Furfural	3.63%
Methanol	32.30%
Cresol	2.90%
Xylenol	1.19%
Guaiacol	2.19%
Methylguaiacol	2.56%
2.3-Dihydropyran	2.24%

Table B.6 - Composition of mesquite sawdust bio-oil [40].

Chemical compound	%molar
Formic acid	3.42%
Acetic acid	10.61%
Pentanoic acid	1.83%
Butanoic acid. 2-hydroxy-	2.88%
Pentanoic acid. 4-methyl-	3.18%
Pentanedioic acid. 3-propyl-	3.59%
Acetic anhydride	1.69%
Vinyl acetate	4.00%
Methyl butanoate	1.50%
Allyl acetylacetate	1.50%
2-Butenal	4.24%
2-Pentanone	2.53%
Octanal	1.79%
Cyclopentenone. 2-hydroxy-3-methyl-	1.63%
Furfural	5.26%
Methanol	25.96%
Levoglucosane	1.50%
Cresol	2.27%
Xylenol	2.16%
Guaiacol	3.27%
Methylguaiacol	5.94%
Methoxycatechol	1.48%
Ethylguaiacol	1.21%
Syringol	2.16%
Benzoic acid. 4-hydroxy-3-methoxy-	0.95%
2.3-Dihydropyran	3.45%

Table B.7 - Composition of wheat shell bio-oil [40].

Chemical compound	%molar
Formic acid	2.55%
Acetic acid	6.79%
Isocrotonic acid	1.05%
Pentanoic acid	1.74%
Butanoic acid. 2-hydroxy-	1.04%
Pentanoic acid. 4-methyl-	1.35%
Pentanedioic acid. 3-propyl-	1.14%
Acetic anhydride	1.06%
Vinyl acetate	2.02%
Methyl butanoate	1.35%
2-Propenyl butanoate	1.33%
Allyl acetylacetate	0.99%
2-Butenal	2.64%
2-Pentanone	1.91%
Cyclopentanone	2.28%
Cyclopentenone. 2-methyl-	1.83%
Cyclopentenone. 2-hydroxy-3-ethyl-	1.74%
Methanol	19.24%
Levoglucosane	3.46%
Cresol	2.95%
Xylenol	7.82%
Guaiacol	4.55%
Methylguaiacol	9.57%
Methoxycatechol	19.59%

Table B.8 - Composition of oil palm shells bio-oil [41].

Chemical Compound	%molar
2-Methyl propane	0.90%
Acetic acid	28.07%
3-Hydroxy 2-propanone	10.48%
2-Methyl pentyl ether	0.82%
Butandial	2.47%
Allyl acetate-2 ene	4.71%
2-Furanaldehyde	4.58%
2-Butanone	1.16%
Methyl crotonate	2.68%
Cyclopentanone	1.59%
Phenol	29.99%
3-Methyl cyclopentanedione	1.23%
2-Methyl phenol	0.73%
2-Methoxy phenol	3.87%
4-Methyl 2-methoxy phenol	1.46%
Catechol	1.96%
4-Ethyl 2-methoxy phenol	0.71%
Syringol	1.78%
4-Propene 2-methoxy phenol	0.82%

Table B.9 - Composition of maple bio-oil [15].

Chemical compound	%molar
Acetic acid	19.24%
Formic acid	27.70%
Hydroxyacetaldehyde	25.22%
Glyoxal	6.18%
Methylglyoxal	1.80%
Formaldehyde	7.96%
Acetol	3.23%
Ethylene glycol	1.93%
Levoglucosan	3.44%
Frutose	1.66%
Glucose	0.66%
Cellobiosan	0.98%

Table B.30 - Composition of oak bio-oil [15].

Chemical compound	%molar
Acetic acid	20.54%
Formic acid	17.69%
Hydroxyacetaldehyde	17.67%
Glyoxal	12.76%
Formaldehyde	18.08%
Acetol	6.00%
Levoglucosan	5.78%
Xylose	1.48%

Table B.4 - Composition of eucalyptus wood bio-oil [42].

Chemical Compounds	% molar
Hydroxy acetone	16.63%
1-Hydroxy-2-butanone	1.28%
1.3-Cyclopentanedione	2.24%
3-Methyl-1.2-Cyclopentanedione	1.40%
Acetic acid	48.23%
Furfural	4.12%
Guaiacol	0.96%
Syringol	1.96%
4-Hydroxy-3-methoxybenzoic acid	2.06%
Vanillin	1.82%
4-Allylsyringol	2.43%
Syringaldehyde	0.86%
Levoglucosan	16.01%

Appendix C

In this appendix the graphical representations of the sub-products (CO, CO_2, CH_4 and coke) will be presented for the different reactor configurations.

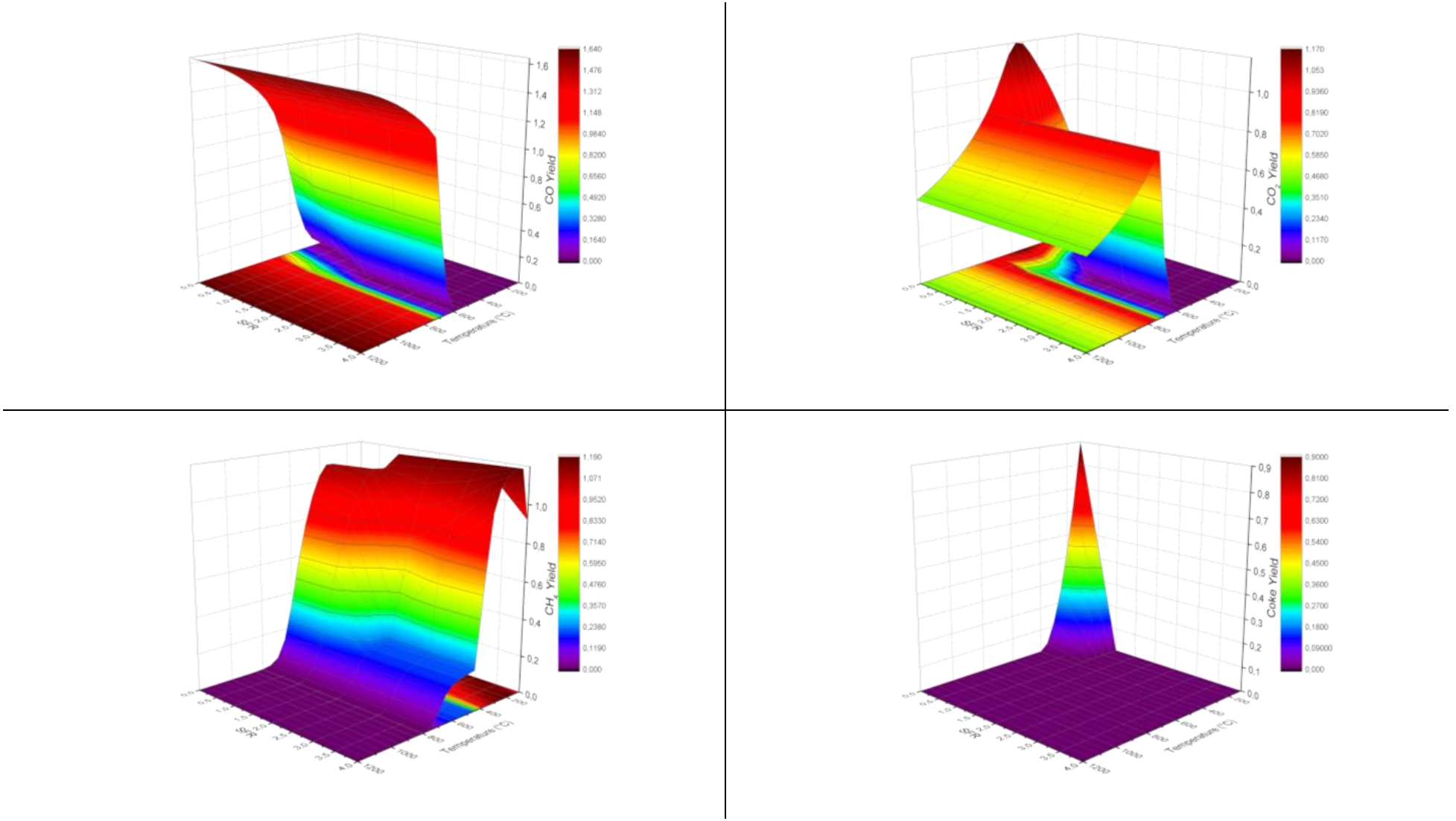

Figure C.1 – Sub-products yield as a function of temperature and SFR for spruce bio-oil at stoichiometric WFR and 1 atm in a SER.

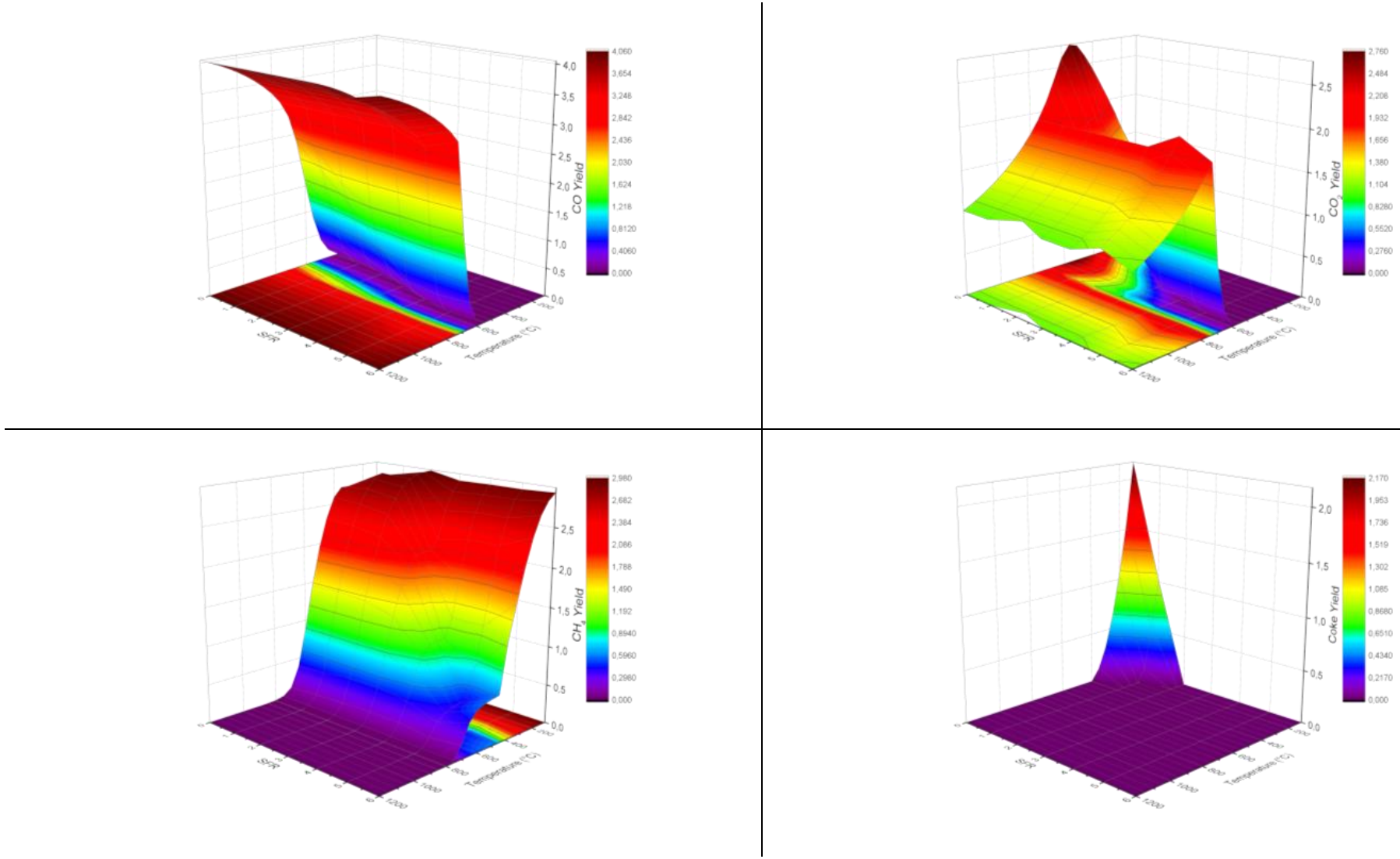

Figure C.2 – Sub-products yield as a function of temperature and SFR for wheat bio-oil at stoichiometric WFR and 1 atm in a SER.

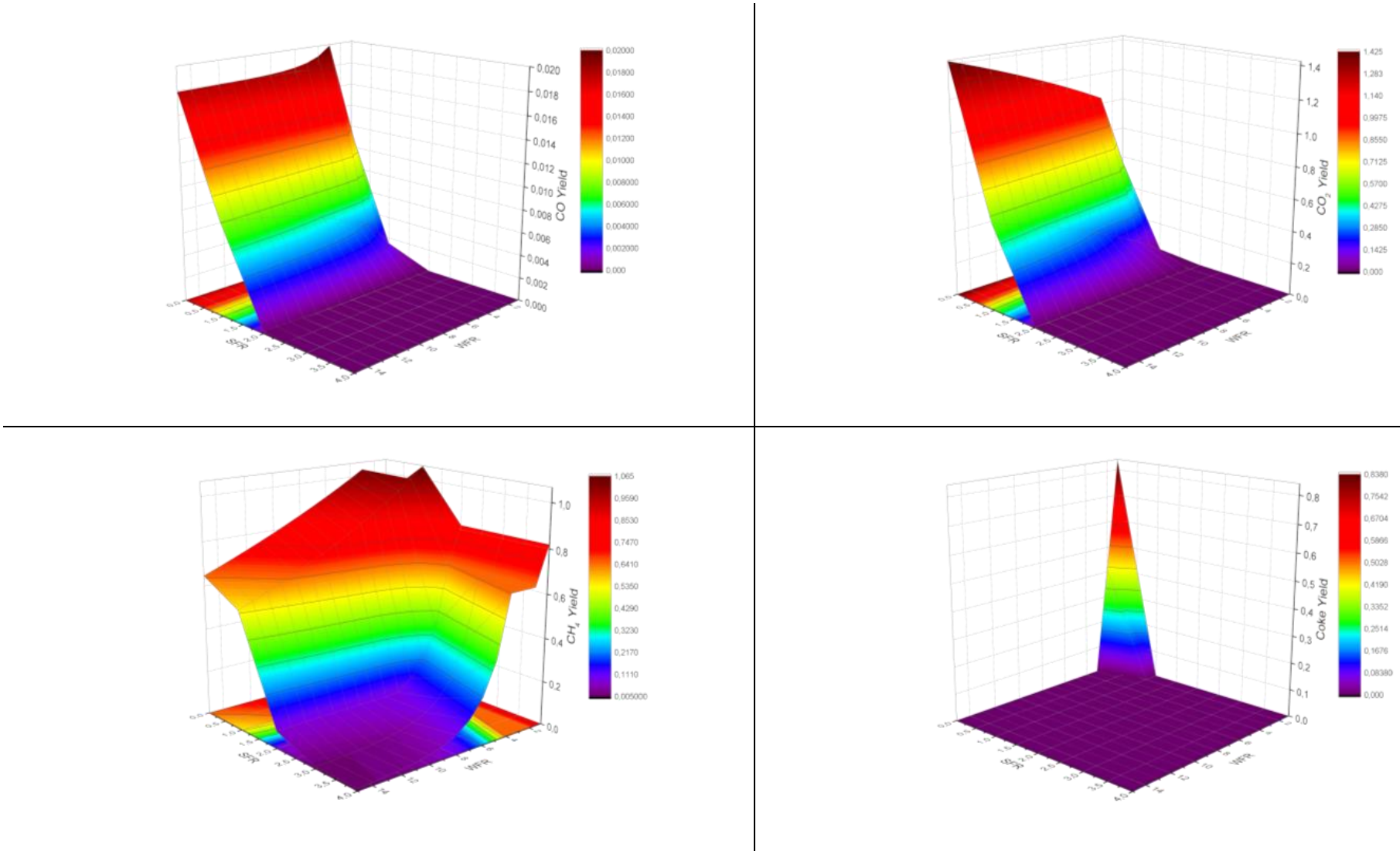

Figure C.3 – Sub-products yield as a function of WFR and SFR for spruce bio-oil at 400 ºC and 1 atm in a SER.

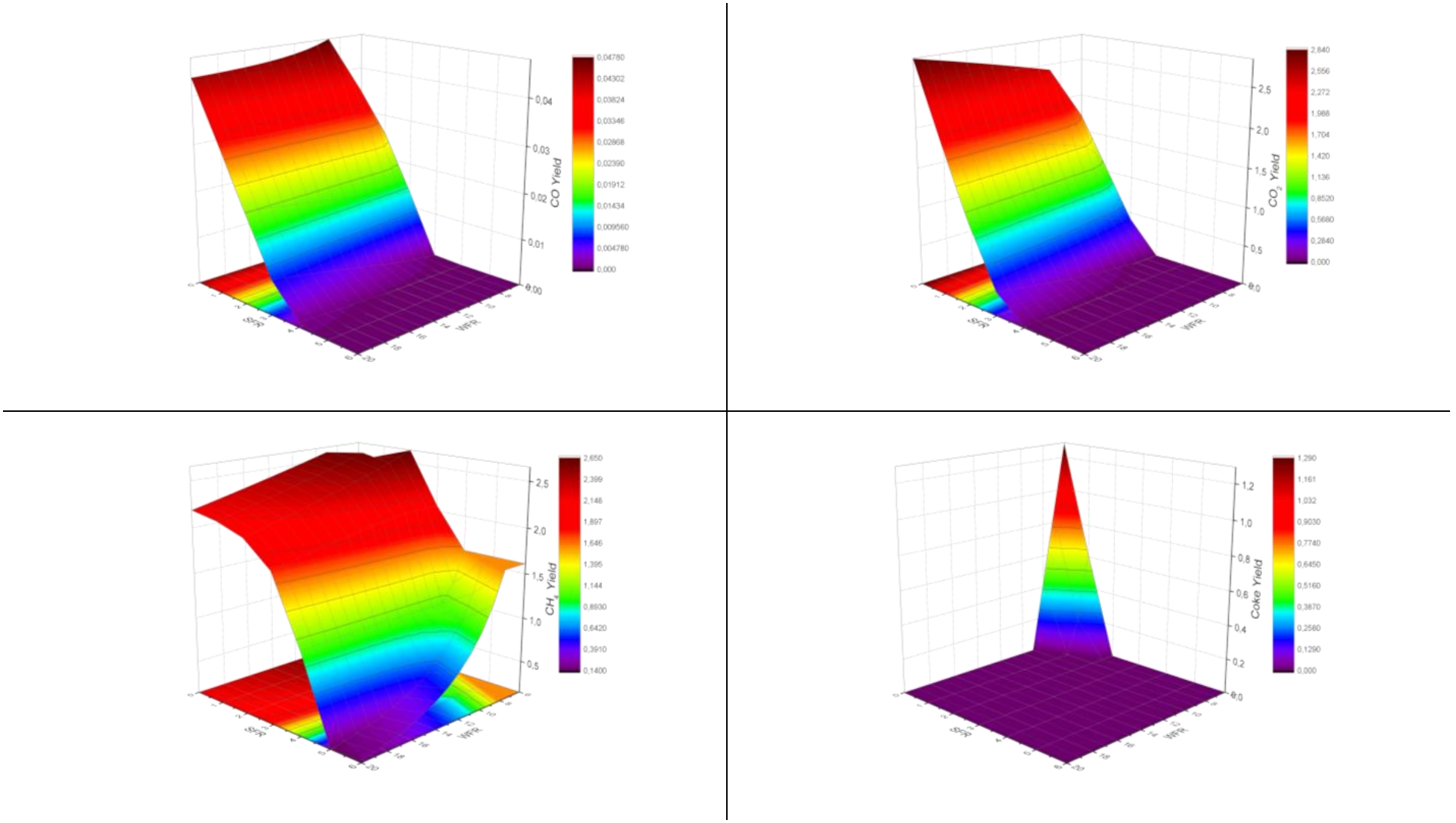

Figure C.4 – Sub-products yield as a function of WFR and SFR for wheat bio-oil at 400 ºC and 1 atm in a SER.

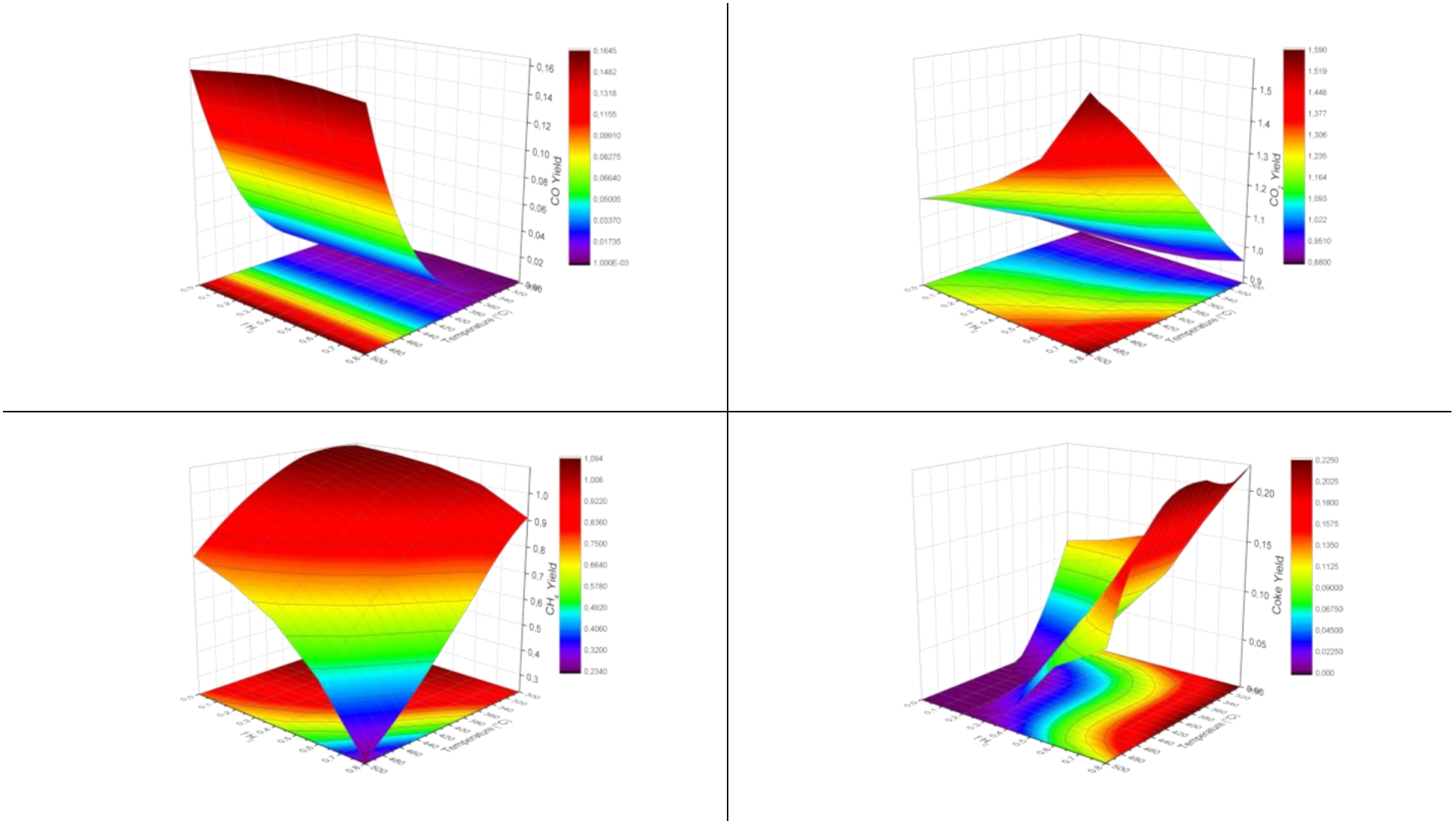

Figure C.5 – Sub- products yield as a function of temperature and hydrogen removal fraction for spruce bio-oil at stoichiometric WFR and 1 atm in a MR.

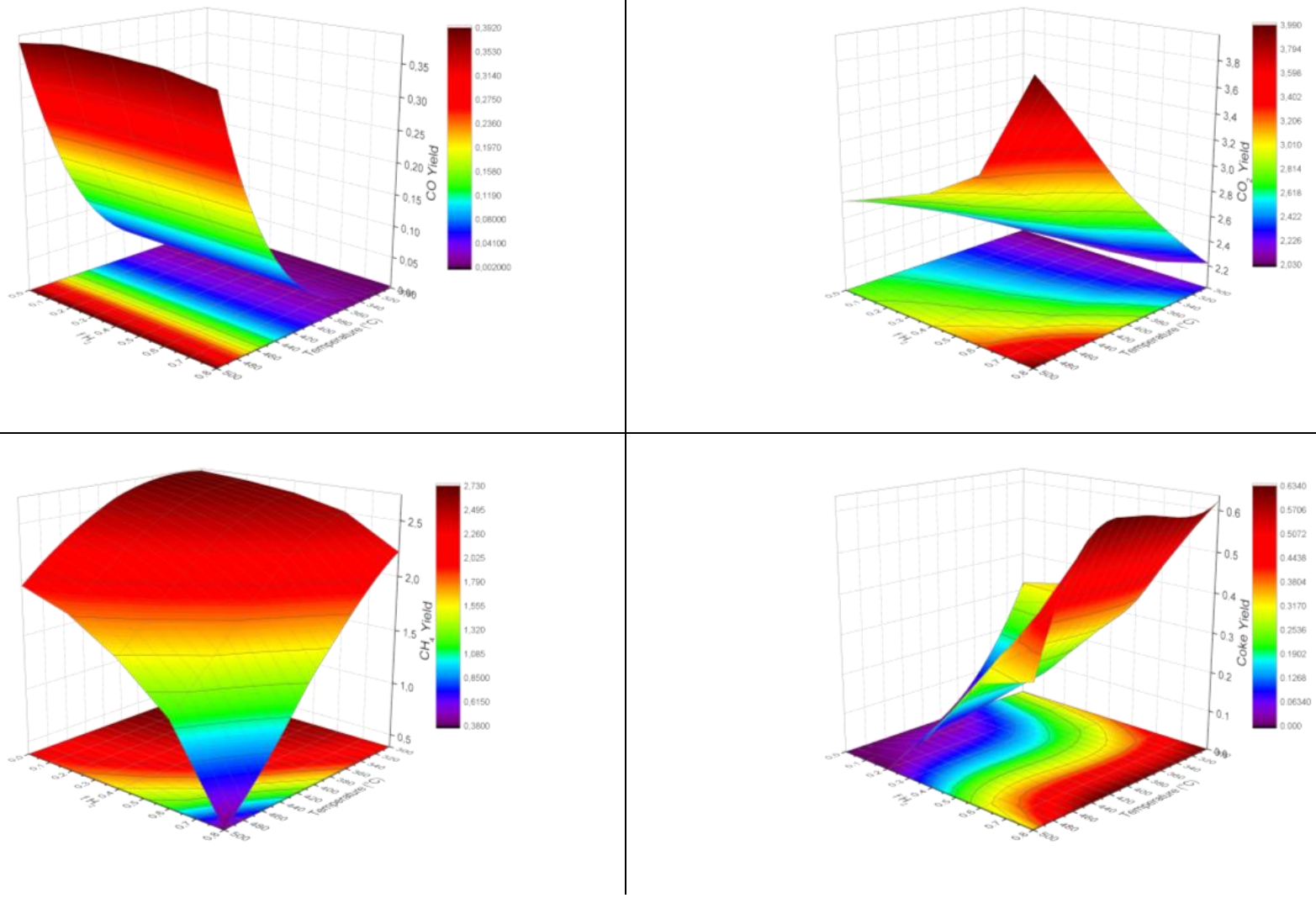

Figure C.6 – Sub- products yield as a function of temperature and hydrogen removal fraction for wheat bio-oil at stoichiometric WFR and 1 atm in a MR.

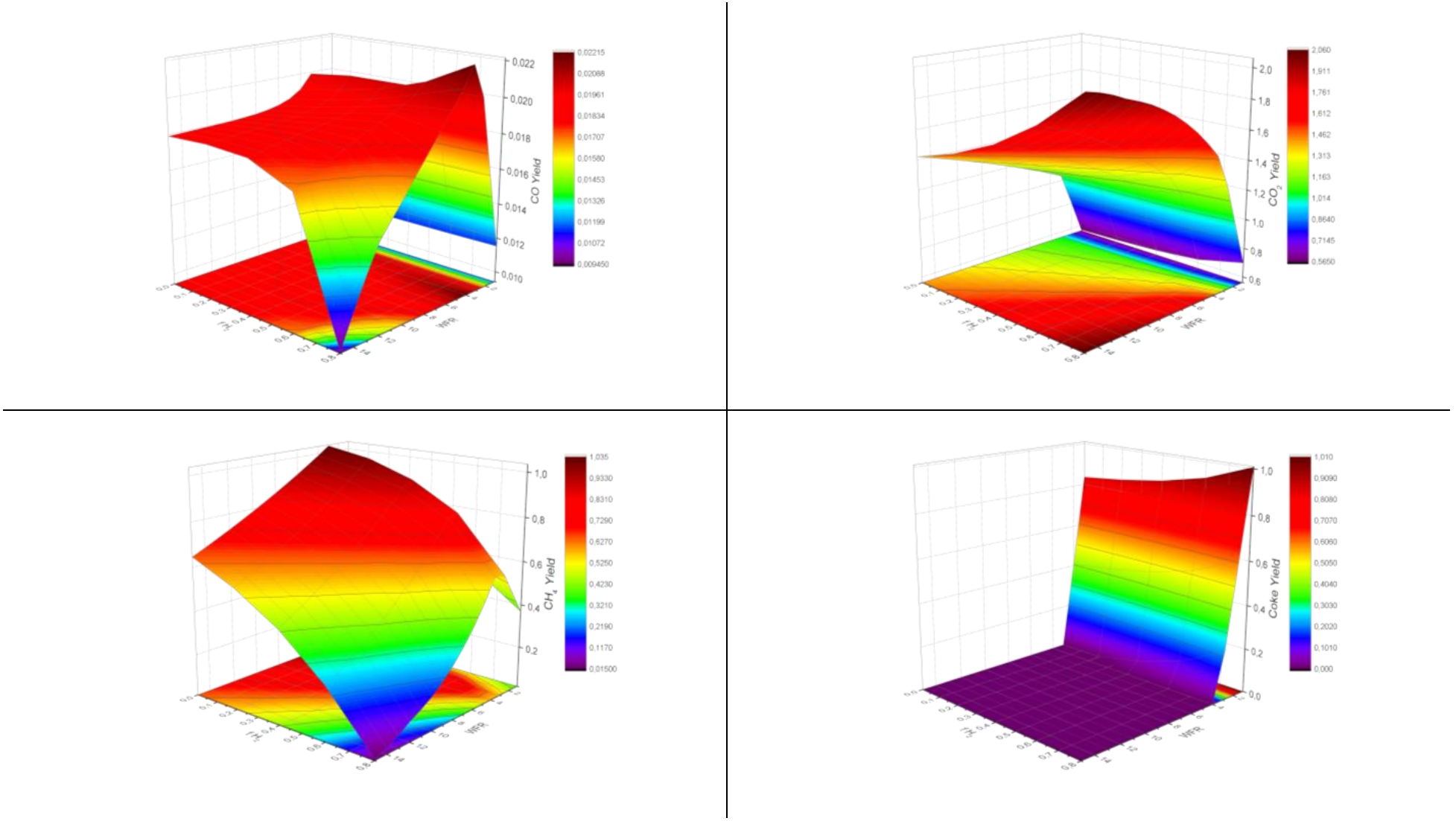

Figure C.7 – Sub-products yield as a function of WFR and hydrogen removal fraction for spruce bio-oil at 400 ºC and 1 atm in a MR.

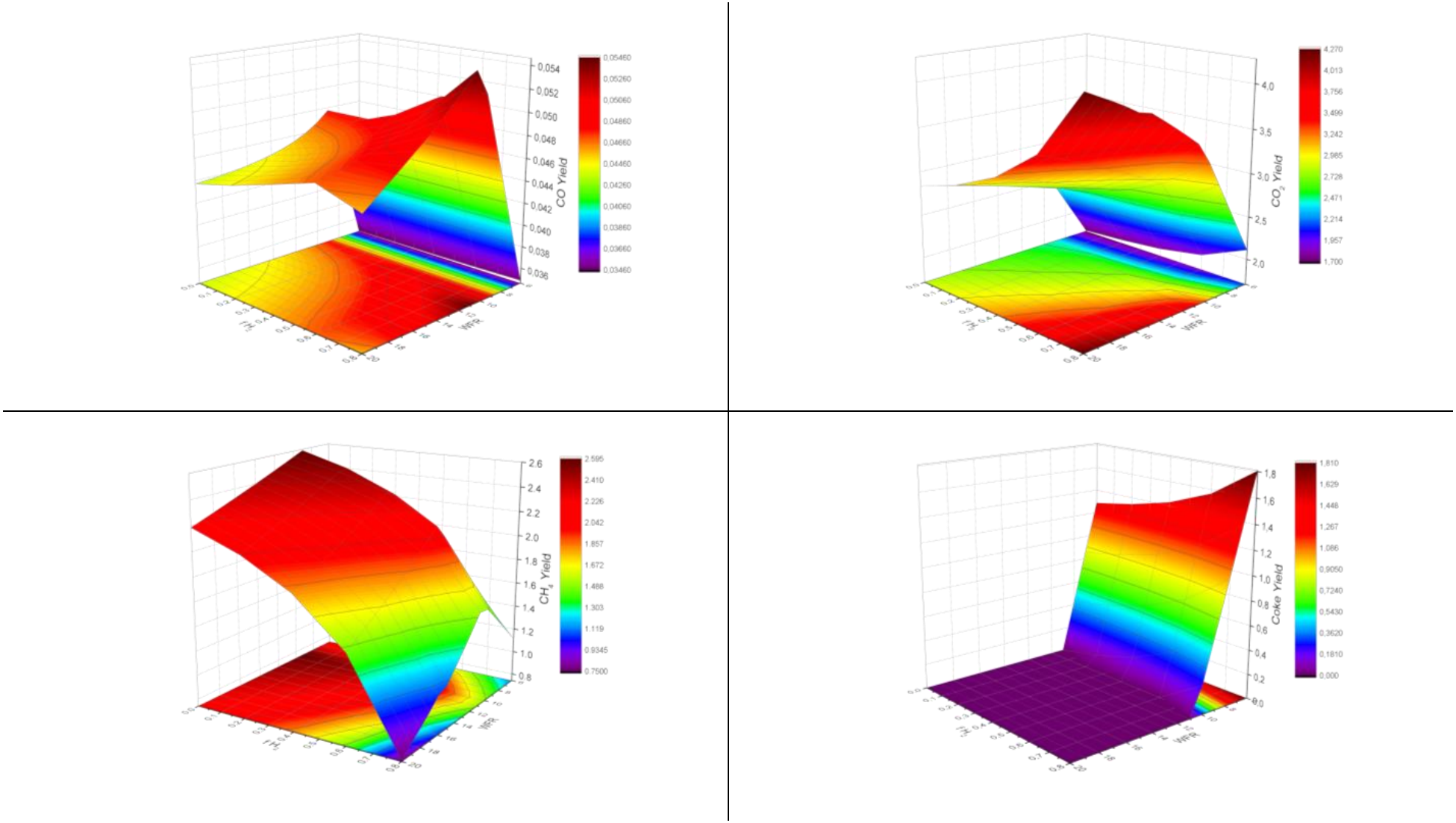

Figure C.8 – Sub- products yield as a function of WFR and hydrogen removal fraction for wheat bio-oil at 400 ºC and 1 atm in a MR.

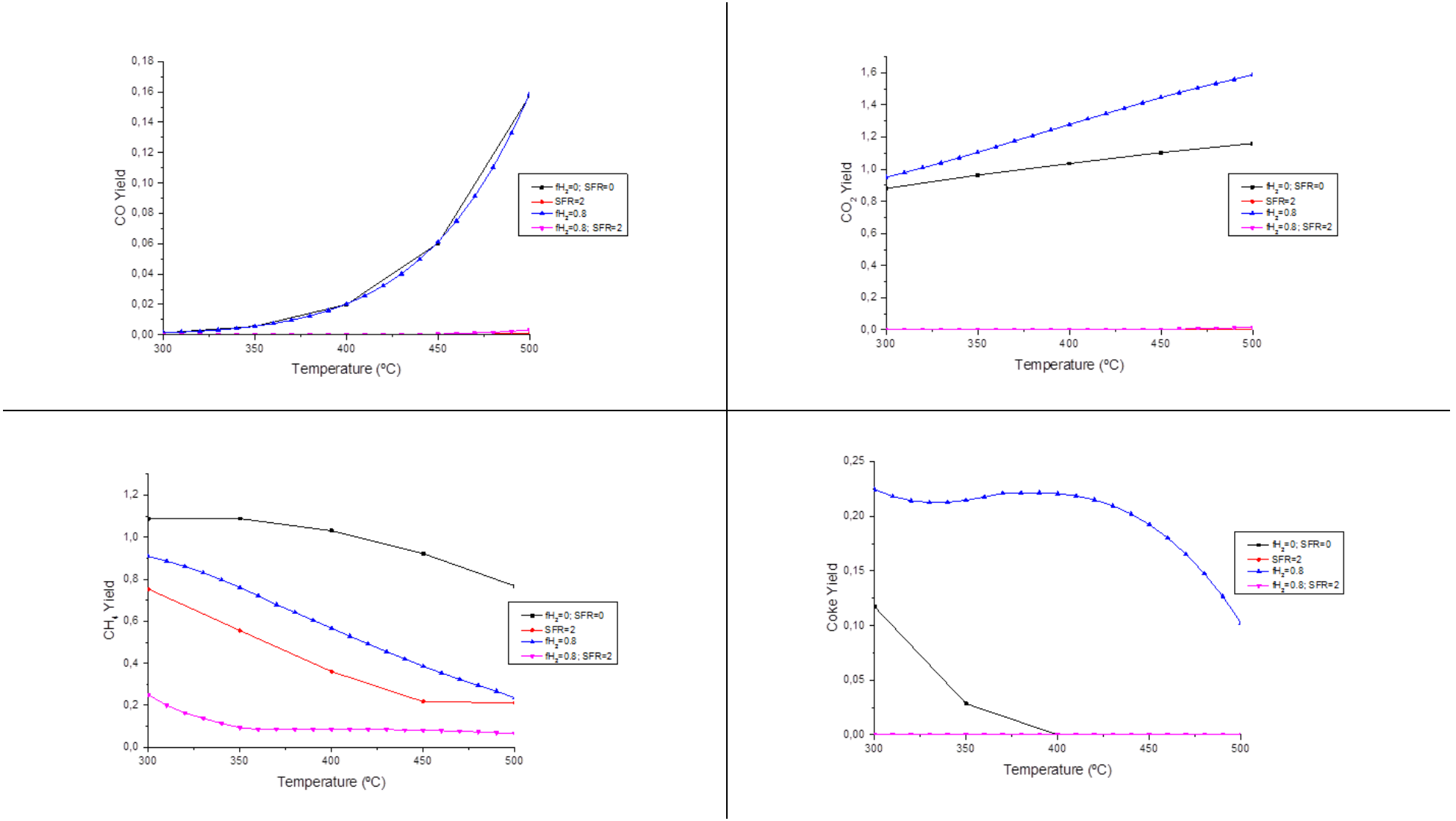

Figure C.9 – Comparison of sub-products yield as a function of temperature for spruce bio-oil in different reactor configurations at stoichiometric WFR and 1 atm.

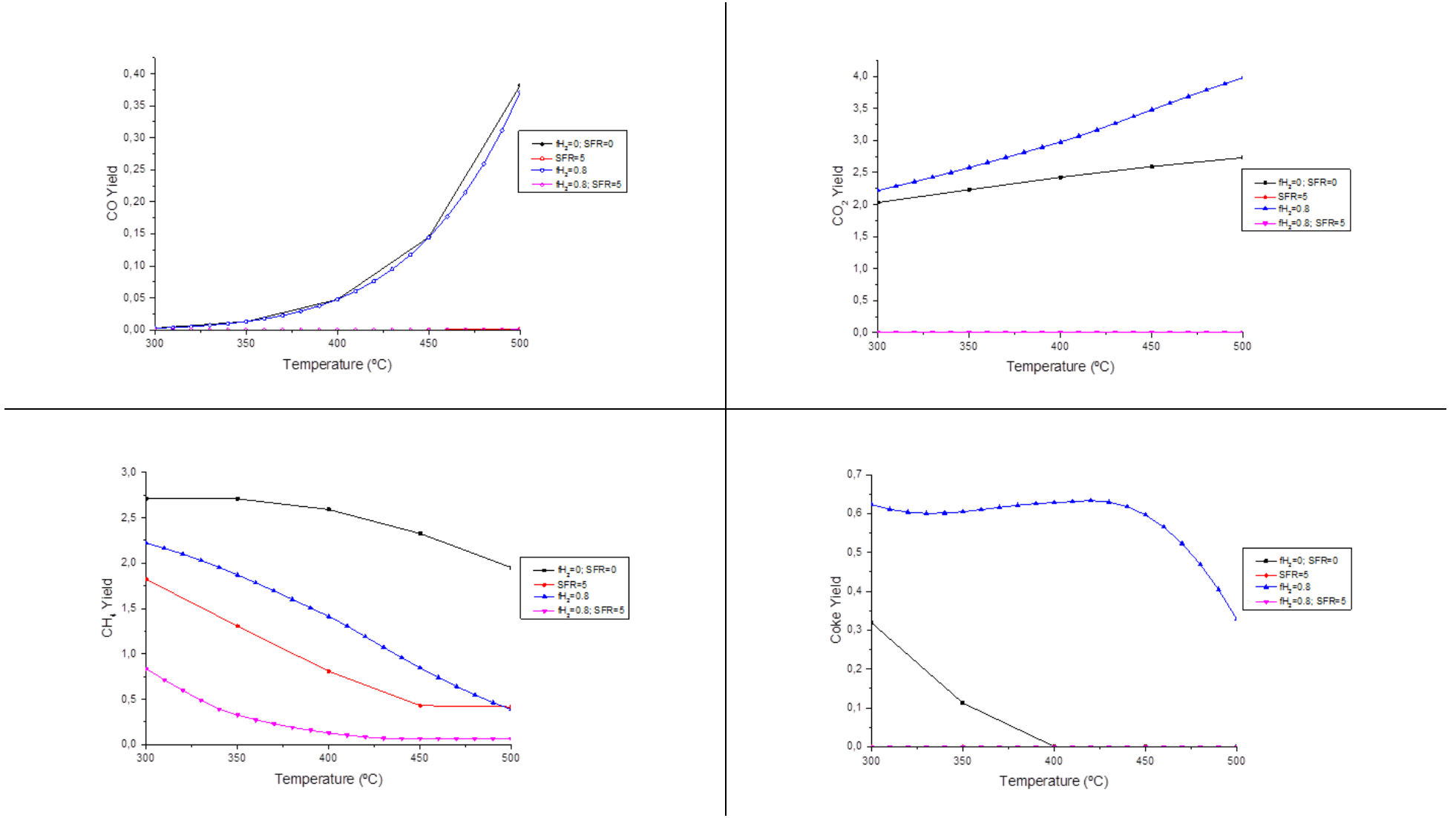

Figure C.10 – Comparison of sub-products yield as a function of temperature for wheat bio-oil in different reactor configurations at stoichiometric WFR and 1 atm.

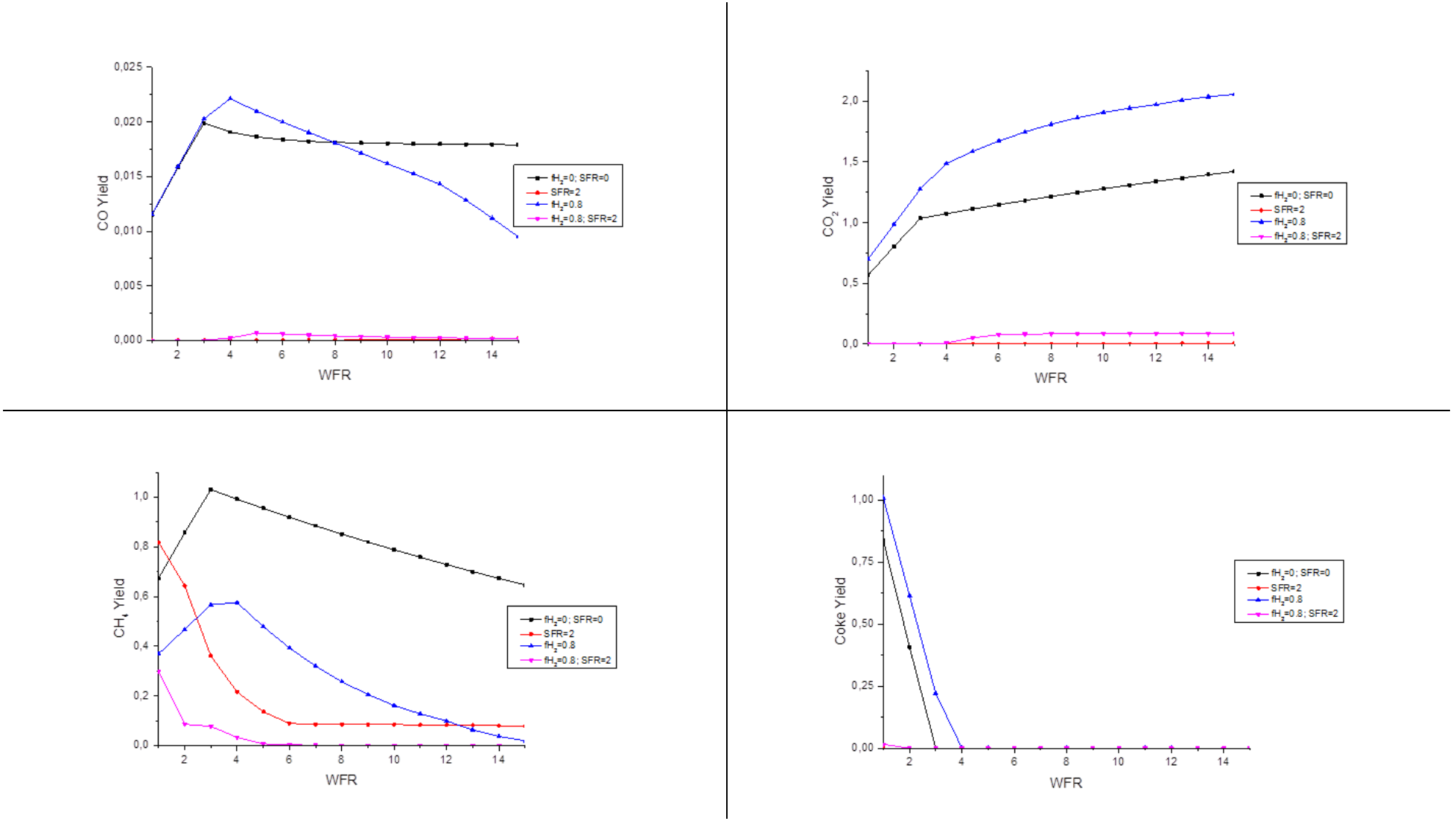

Figure C.11 – Comparison of sub-products yield as a function of the water to feed molar ratio (WFR) for spruce bio-oil in different reactor configurations at 400 ºC and 1 atm.

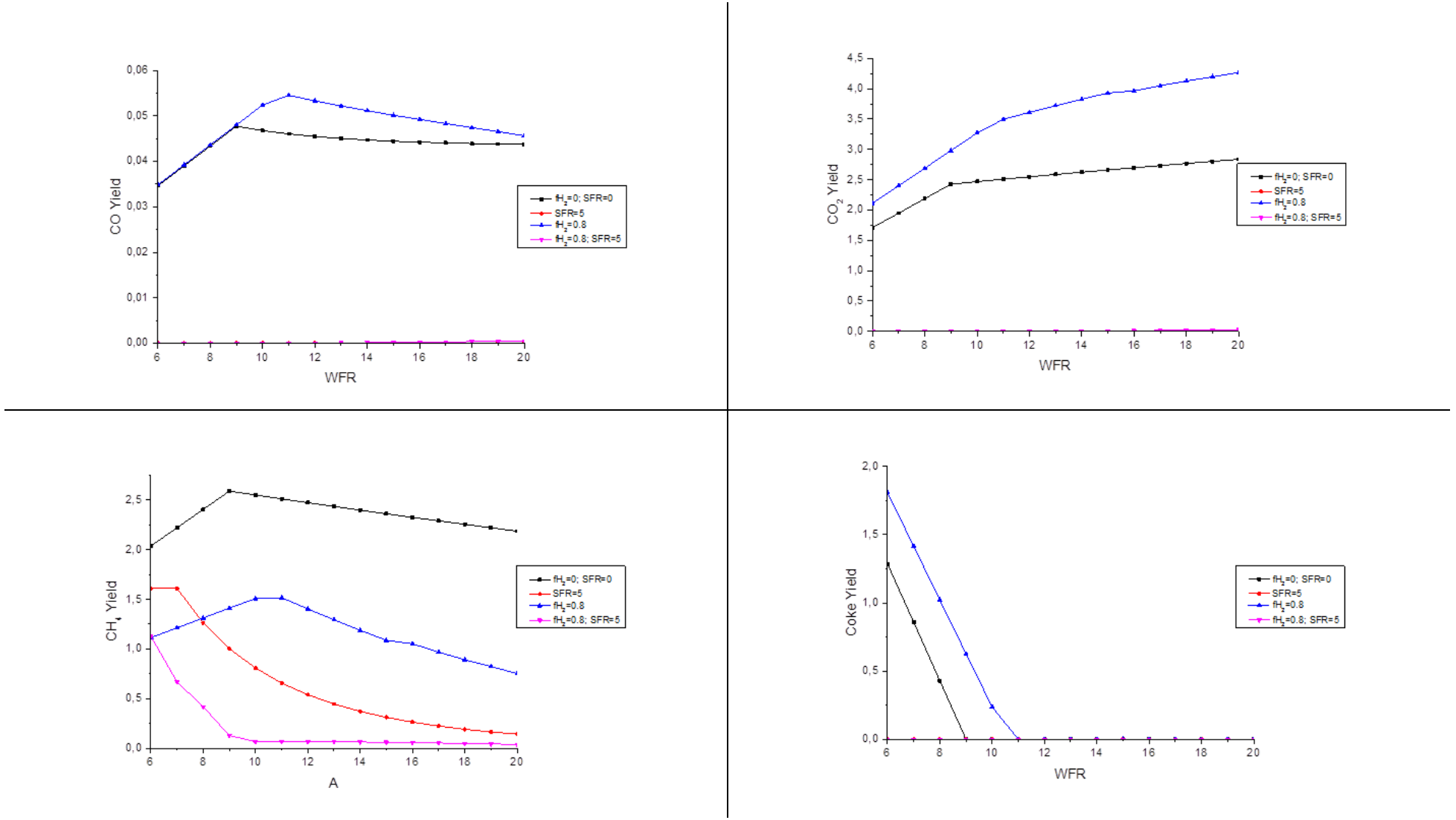

Figure C.12 – Comparison of sub-products yield as a function of the water to feed molar ratio (WFR) for wheat bio-oil in different reactor configurations at 400 ºC and 1 atm.